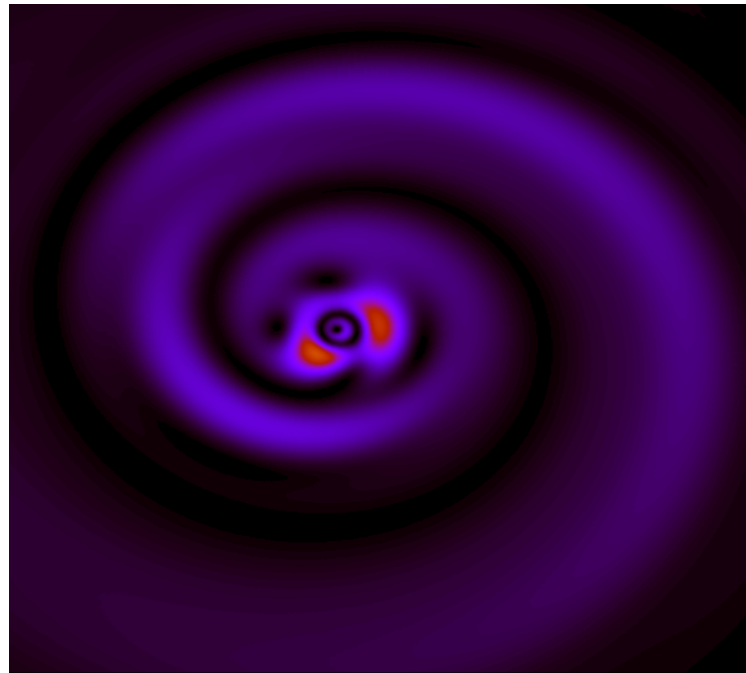
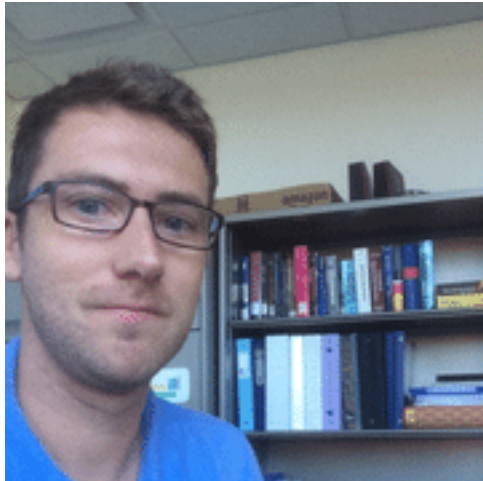


Coherent Control and Attosecond Dynamics with Pulsed XUV and IR Radiation

Nicolas Douguet and Klaus Bartschat

Drake University, Des Moines, IA 50311, USA



XSEDE

Extreme Science and Engineering
Discovery Environment

NSF support under PHY-1430245 and XSEDE-090031

Overview of the Talk

1. Light-induced Coherent Quantum Control

- (a) Interfering **one-photon** and **two-photon** ionization by XUV femtosecond pulses.
- (b) Overlapping XUV pulses with an **optical field** (XUV + IR).
- (c) Using **circularly polarized** XUV femtosecond pulses.

Overview of the Talk

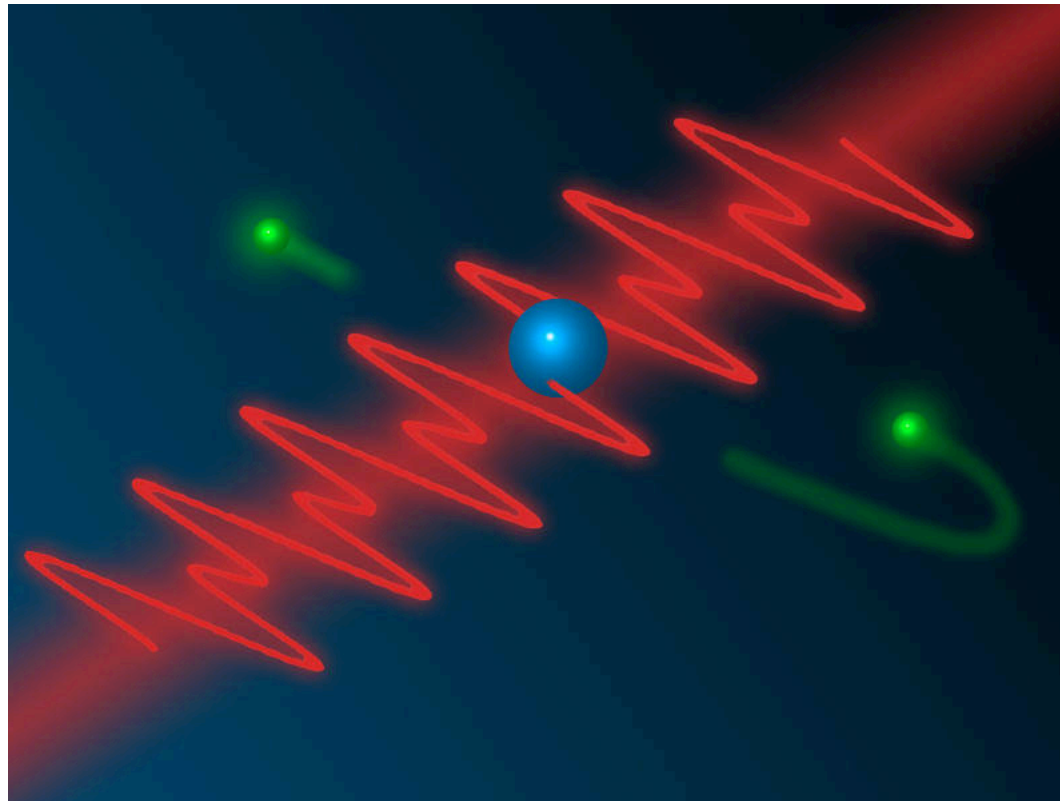
1. Light-induced Coherent Quantum Control

- (a) Interfering **one-photon** and **two-photon** ionization by XUV femtosecond pulses.
- (b) Overlapping XUV pulses with an **optical field** (XUV + IR).
- (c) Using **circularly polarized** XUV femtosecond pulses.

2. Multiphoton and Tunneling Ionization

- (a) **Circular dichroism** in two-color resonant multiphoton ionization of oriented He^+ .
(Additional theoretical predictions; complementary to M. Ilchen's talk)
- (b) Attoclock studies of **tunneling time**.
- (c) Interpretation using **Bohmian Mechanics** (if time allows)

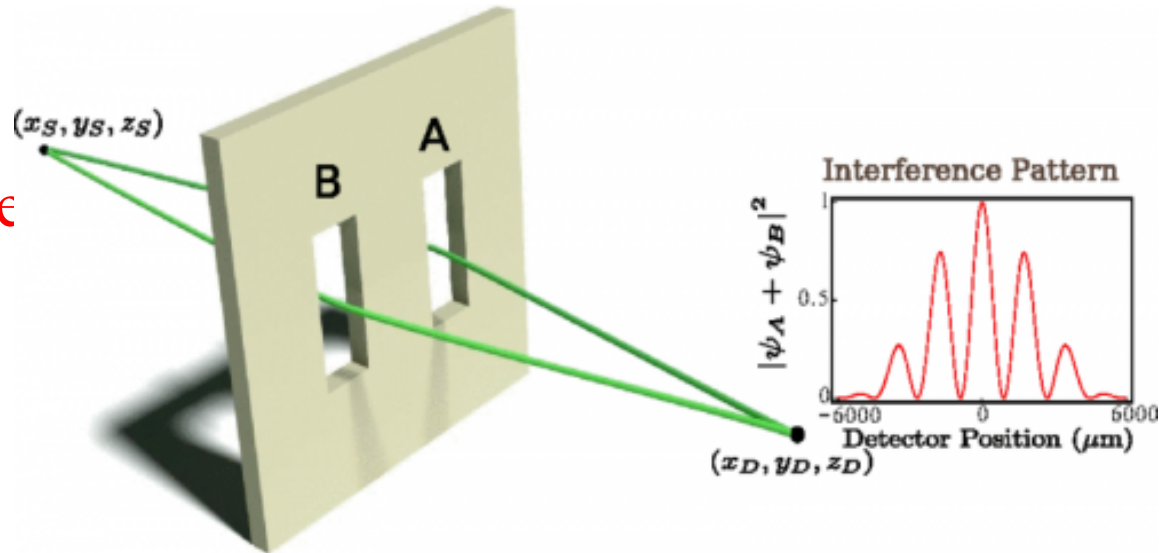
Light-induced Coherent Quantum Control



Motivation

- One of the goals of “quantum control” is to steer electrons into specific directions or locations (e.g., selected bond breaking in a molecule).

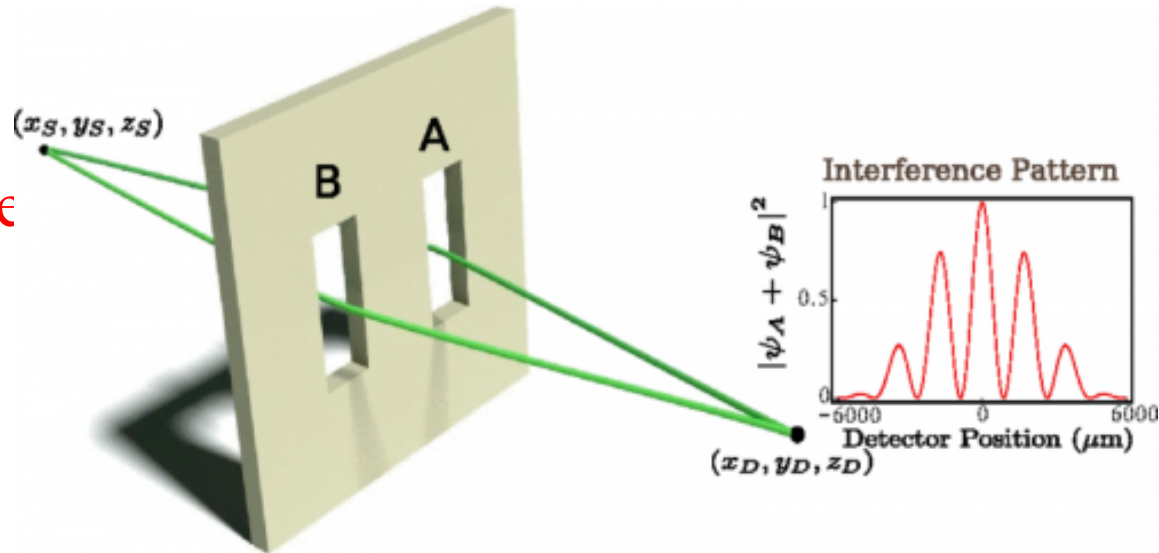
- Two-pathways interference is a way to achieve coherent control.



Motivation

- One of the goals of “quantum control” is to steer electrons into specific directions or locations (e.g., selected bond breaking in a molecule).

- Two-pathways interference is a way to achieve coherent control.

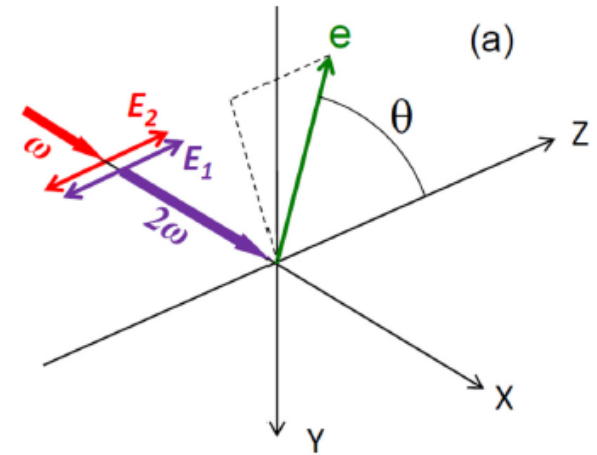


- Photoionization of an atomic system by the fundamental and the second harmonic ($\omega + 2\omega$) of a femtosecond VUV pulse is an example of coherent control of the photoelectron angular distribution.

Bichromatic Atomic Ionization with Linearly Polarized Light

- In the case of linearly polarized light, the electric field is expressed as

$$E(t) = F(t) [\cos \omega t + \eta \cos(2\omega t + \phi)]$$

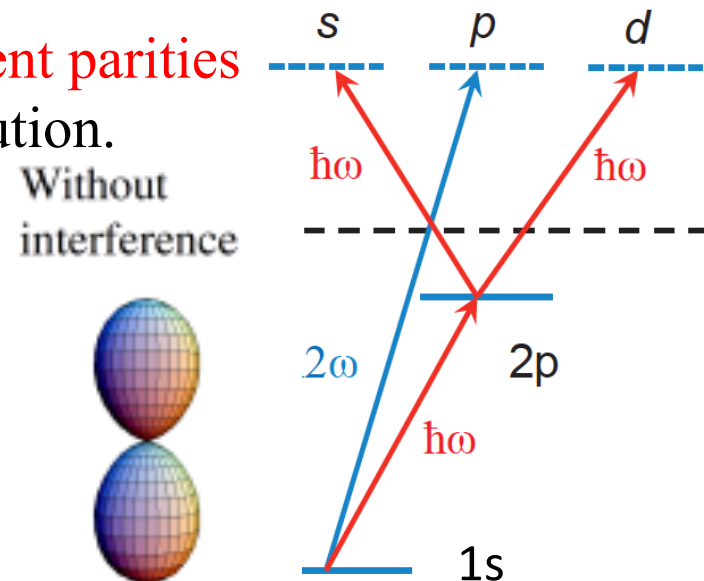
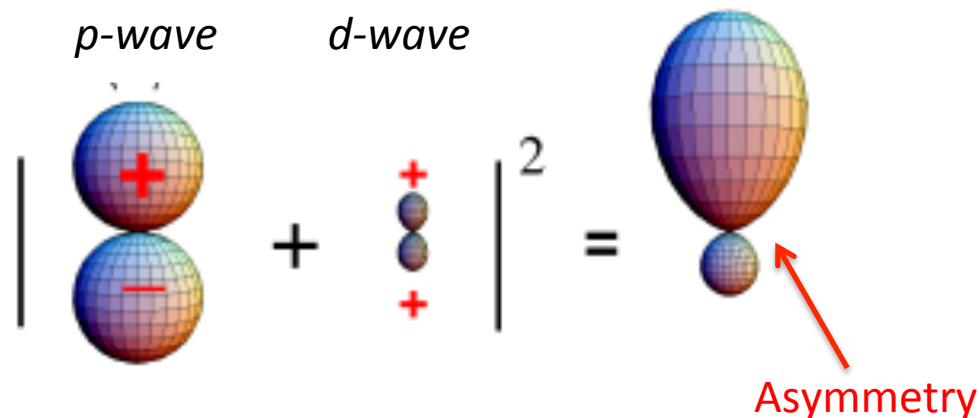
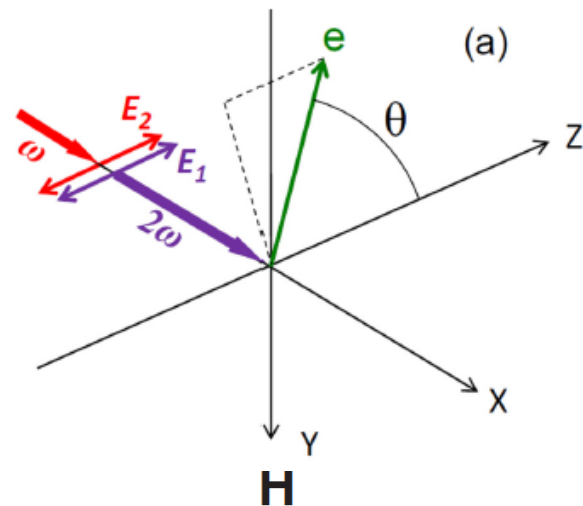


Bichromatic Atomic Ionization with Linearly Polarized Light

- In the case of linearly polarized light, the electric field is expressed as

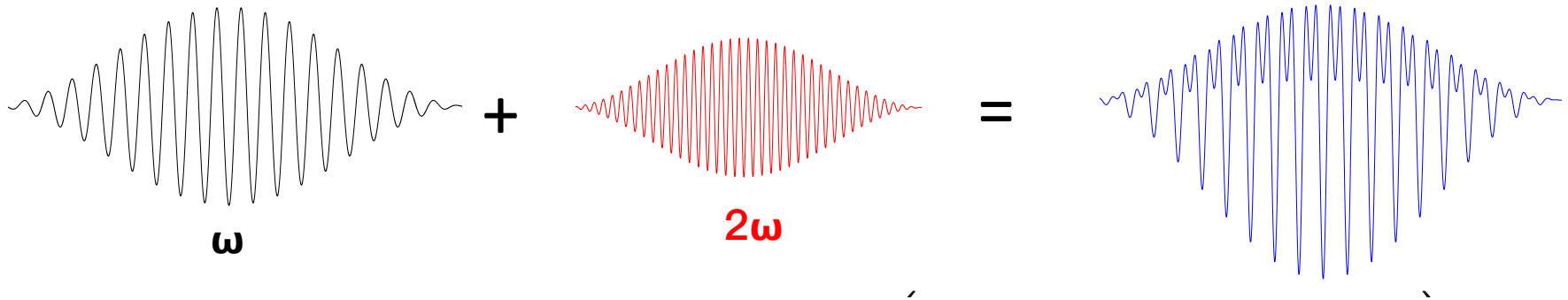
$$E(t) = F(t) [\cos \omega t + \eta \cos(2\omega t + \phi)]$$

- Two-pathways interference** is enhanced by tuning the first harmonic near an intermediate state (e.g. 2p in H).
- Ionization leading to partial waves **with different parities** **can** cause an asymmetry in the angular distribution.



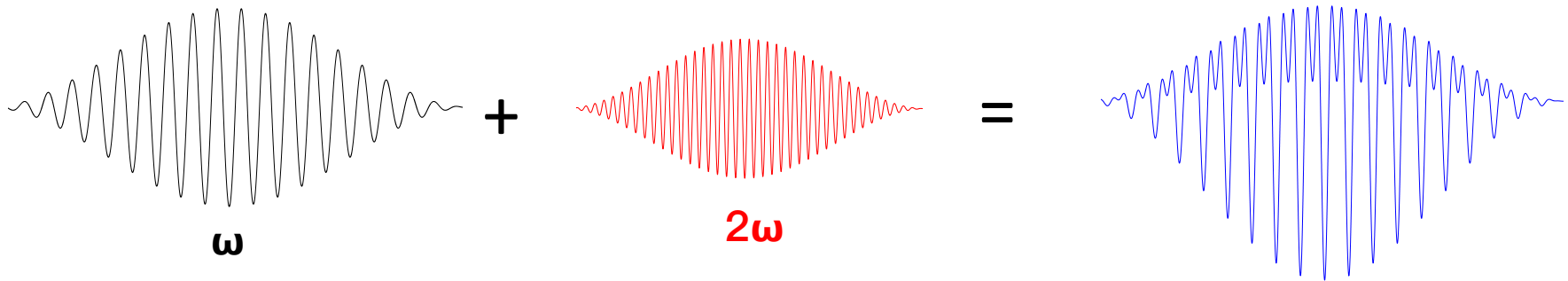
Control of the Photoelectron Angular Distribution (PAD)

- The asymmetry in the PAD is the result of $\langle E^3 \rangle \neq 0$ of the electric field [N. B. Baranova and B. Ya. Zel'dovich, J. Opt. Soc. Am. B 8 27 (1990)].



Control of the Photoelectron Angular Distribution (PAD)

- The asymmetry in the PAD is the result of $\langle E^3 \rangle \neq 0$ of the electric field [N. B. Baranova and B. Ya. Zel'dovich, J. Opt. Soc. Am. B 8 27 (1990)].

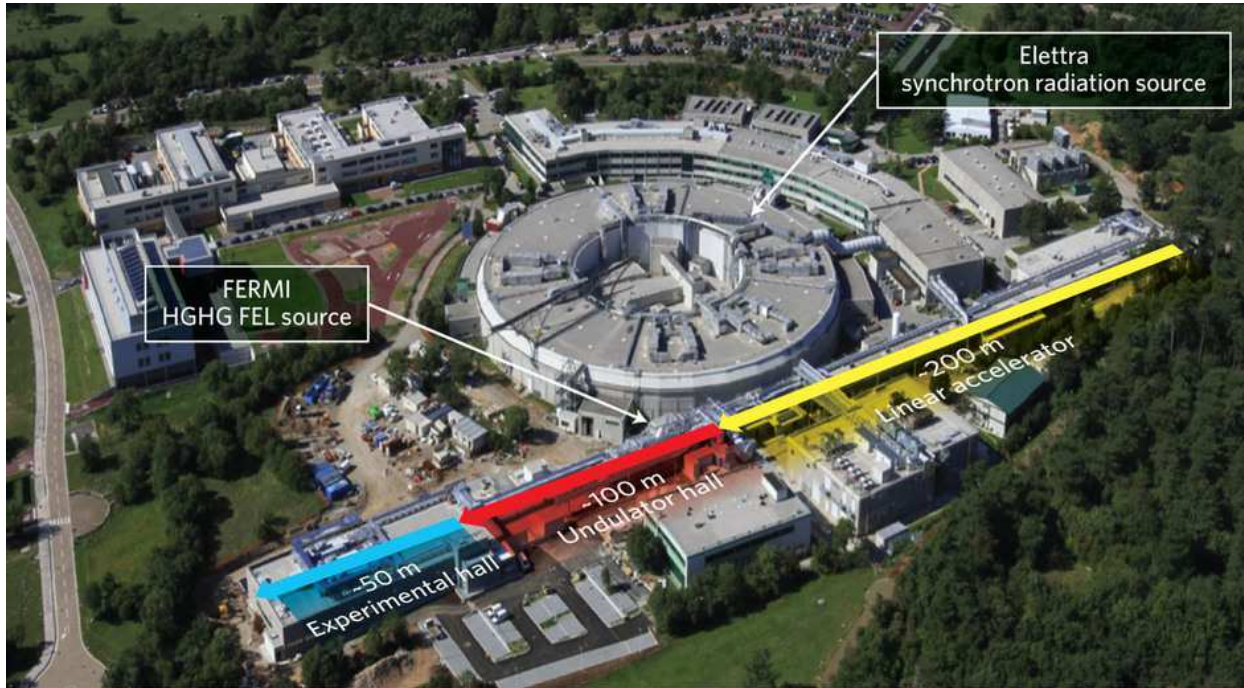


- The PAD takes the form:
$$W(\theta) = \frac{W_0}{4\pi} \left(1 + \sum_k \beta_k P_k(\cos \theta) \right)$$

→ The **odd-rank anisotropy** parameters are responsible for the PAD asymmetry.
- The asymmetry is defined as:

$$A(0) = \frac{W(0) - W(\pi)}{W(0) + W(\pi)} = \frac{\sum_{k=1,3,\dots} \beta_k}{1 + \sum_{k=2,4,\dots} \beta_k}$$

Experimental Setup at FERMI (Trieste, Italy)

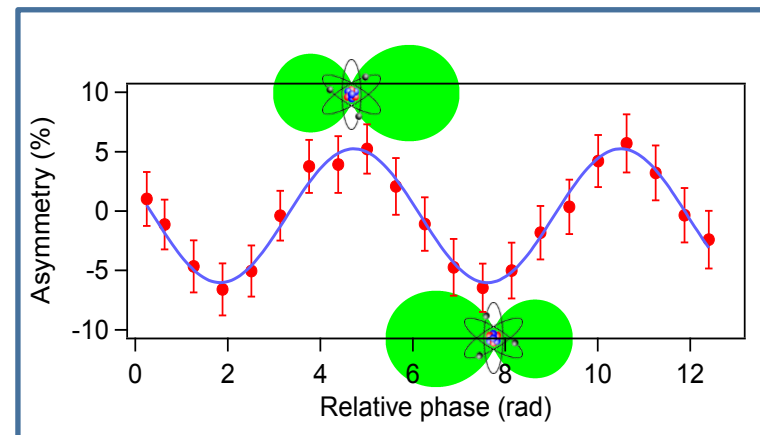


Basic idea: Use $\text{Ne}(2p^6)$ as target and tune the fundamental to one of the $(2p^5 4s)_{J=1}$ states.

Results: (more details at K.C. Prince's ICPEAC Talk)

The delay between the two pulses was controlled to a precision better than **3.1 attoseconds (as)**. This is equivalent to controlling the phase ϕ to high precision [K.C. Prince *et al.*, *Nat. Phot.* **10** (2016) 176-179]

→ The asymmetry oscillates as a function of ϕ as predicted theoretically.



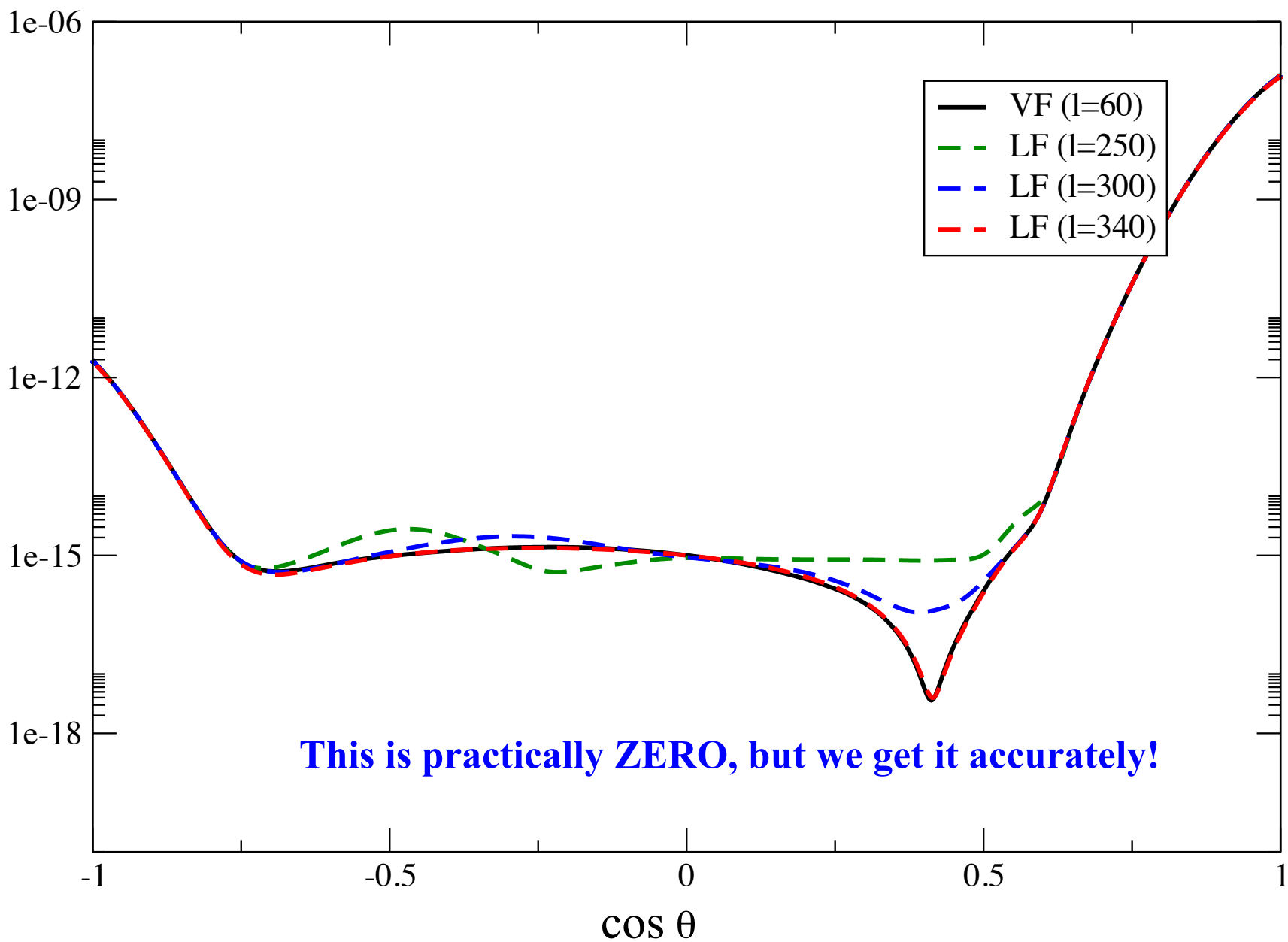
Numerical Approach

- we solve the **Time-Dependent Schrödinger Equation (TDSE)** in the Single-Active Electron (SAE) approach:

$$\hat{H}\Psi(\mathbf{r}, t) = \left(-\frac{\nabla^2}{2} - \frac{1}{r} + \sqrt{\frac{4\pi}{3}} r \sum_{q=0, \pm 1} \mathcal{E}_q^*(t) Y_{1q}(\theta, \varphi) \right) \Psi(\mathbf{r}, t) = i \frac{\partial}{\partial t} \Psi(\mathbf{r}, t)$$

- The wavefunction is expanded in spherical harmonics. We solve the system of coupled equations using **finite differences, split-operator method, series expansion, Crank-Nicolson, matrix iteration, ...**, in both the length and velocity forms of the electric dipole operator, ...
- The numerical issues are by no means trivial, and we spent a lot of time to ensure stability, accuracy, and efficiency.

The Esry-Challenge: 3 cycles, 800 nm, 10^{14} W/cm², PAD at 10 U_p (60 eV)



Numerical Approach

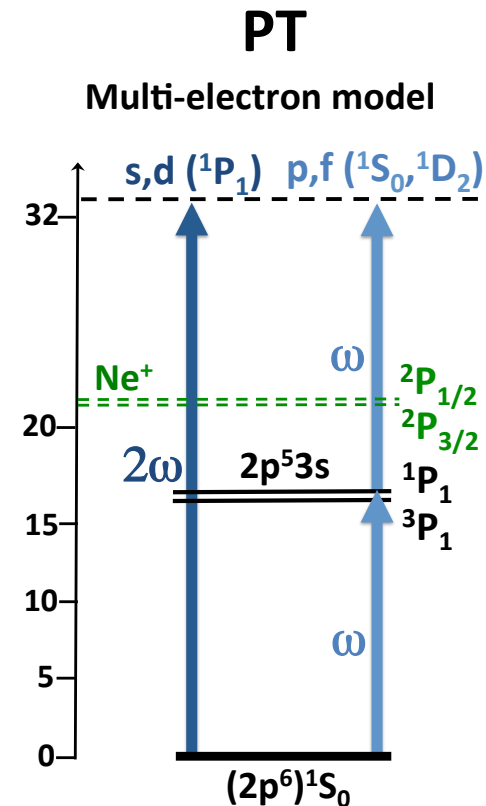
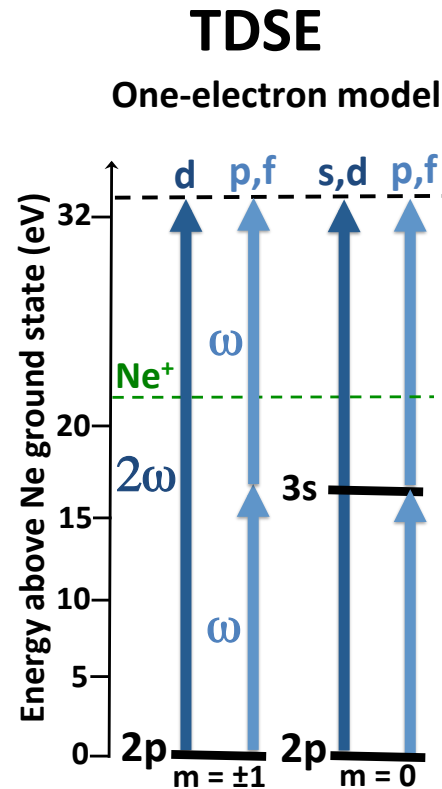
- We solve the **Time-Dependent Schrödinger Equation (TDSE)** in the Single-Active Electron (SAE) approach:

$$\hat{H}\Psi(\mathbf{r}, t) = \left(-\frac{\nabla^2}{2} - \frac{1}{r} + \sqrt{\frac{4\pi}{3}} r \sum_{q=0, \pm 1} \mathcal{E}_q^*(t) Y_{1q}(\theta, \varphi) \right) \Psi(\mathbf{r}, t) = i \frac{\partial}{\partial t} \Psi(\mathbf{r}, t)$$

- The wavefunction is expanded in spherical harmonics. We solve the system of coupled equations using **finite differences, split-operator method, series expansion, Crank-Nicolson, matrix iteration, ...**, in both the length and velocity forms of the electric dipole operator, ...
- The numerical issues are by no means trivial, and we spent a lot of time to ensure stability, accuracy, and efficiency.
- Our colleagues at Moscow State University (A.N. Grum-Grzhimailo, E.V. Gryzlova, E.I. Staroselskaya) use time-dependent **Perturbation Theory (PT)** to obtain the anisotropy parameters calculating the first-order (**one-photon absorption**) and second-order (**two-photon absorption**) ionization amplitudes.

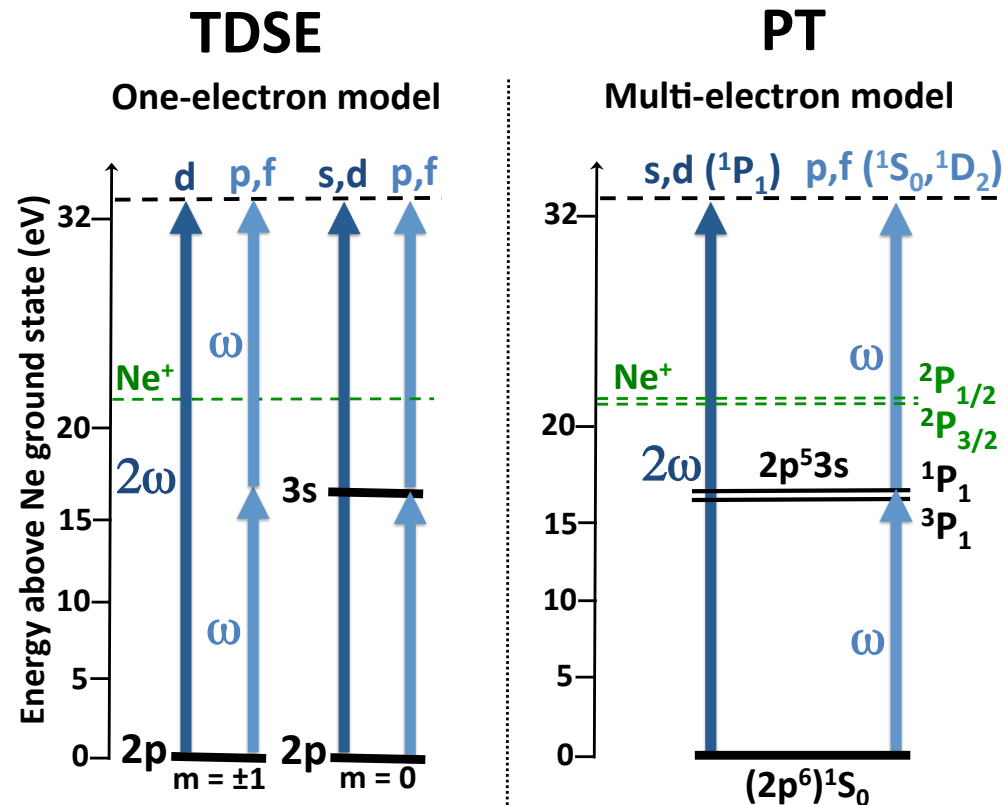
Using $2p^5 3s$ as Intermediate States

- We use the two $(2p^5 3s)$ $J=1$ states as stepping stones to enhance two-photon absorption.
- The TDSE calculations employ a **one-electron** model (no fine-structure), whereas PT uses a **multi-electron model**.
- LS coupling \rightarrow Only one state can be significantly excited.



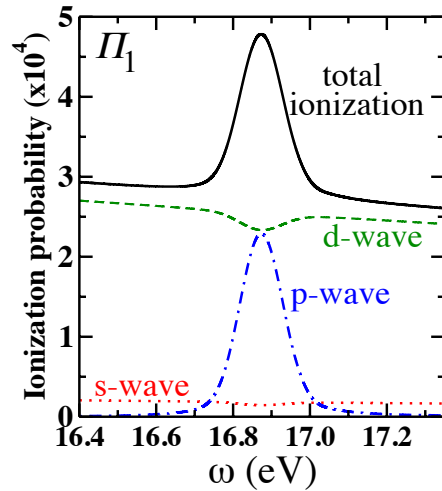
Using $2p^5 3s$ as Intermediate States

- We use the two $(2p^5 3s) J=1$ states as stepping stones to enhance two-photon absorption.
- The TDSE calculations employ a **one-electron** model (no fine-structure), whereas PT uses a **multi-electron model**.
- LS coupling \rightarrow Only one state can be significantly excited.
- Using PT we can obtain analytical expressions for the angular distribution and the anisotropy parameters $\beta_1, \beta_2, \beta_3$, and β_4 . This allows to scan the parameter space efficiently.
- So it's important to know whether PT is reliable.



Theoretical Predictions

- We consider pulses of the form $E(t) = F(t) [\cos \omega t + \eta \cos(2\omega t + \phi)]$ with sine-squared pulse envelope $F(t)$ and fundamental peak intensity $I = 10^{12} \text{ W/cm}^2$.

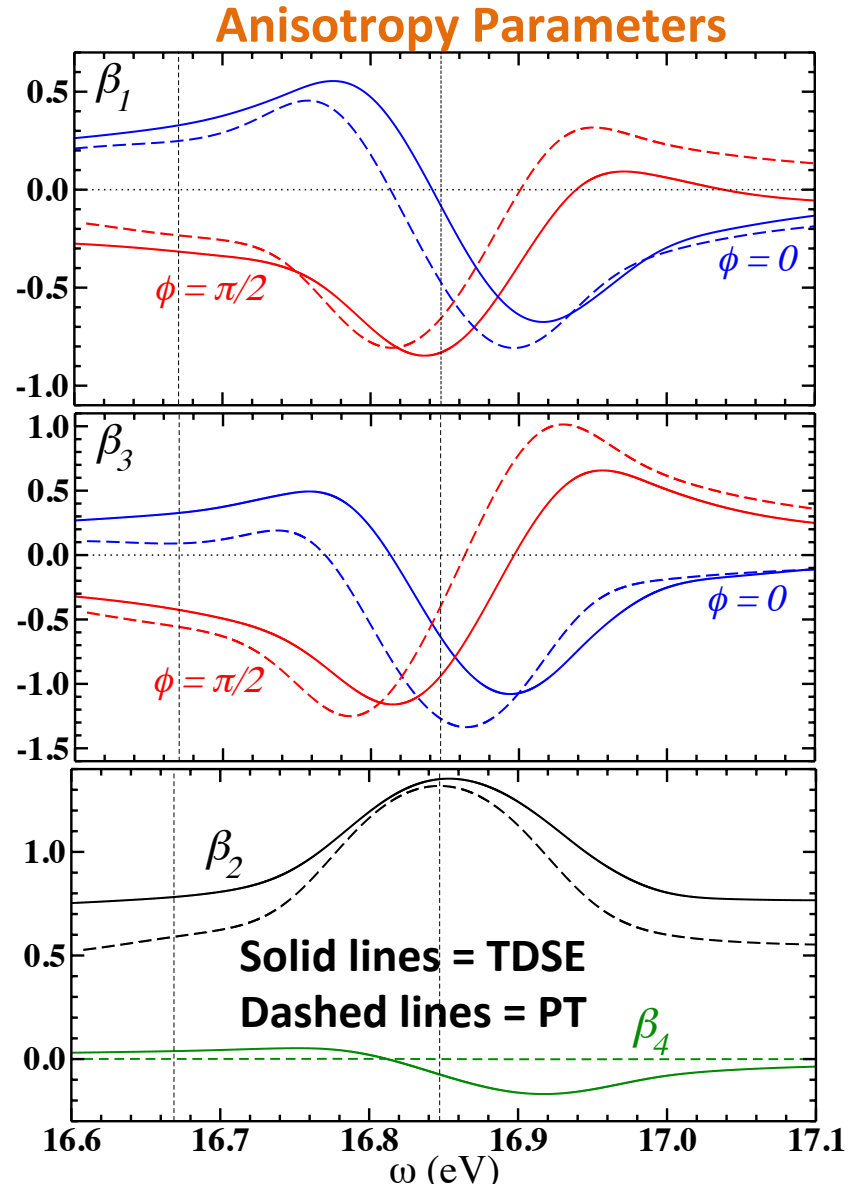
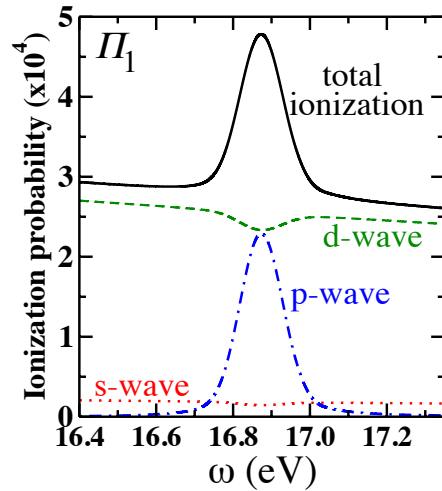


Partial-wave
ionization
probability

Theoretical Predictions

- We consider pulses of the form $E(t) = F(t) [\cos \omega t + \eta \cos(2\omega t + \phi)]$ with sine-squared pulse envelope $F(t)$ and fundamental peak intensity $I = 10^{12} \text{ W/cm}^2$.

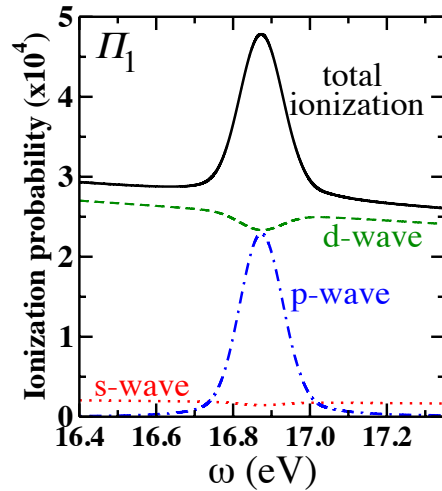
Partial-wave ionization probability



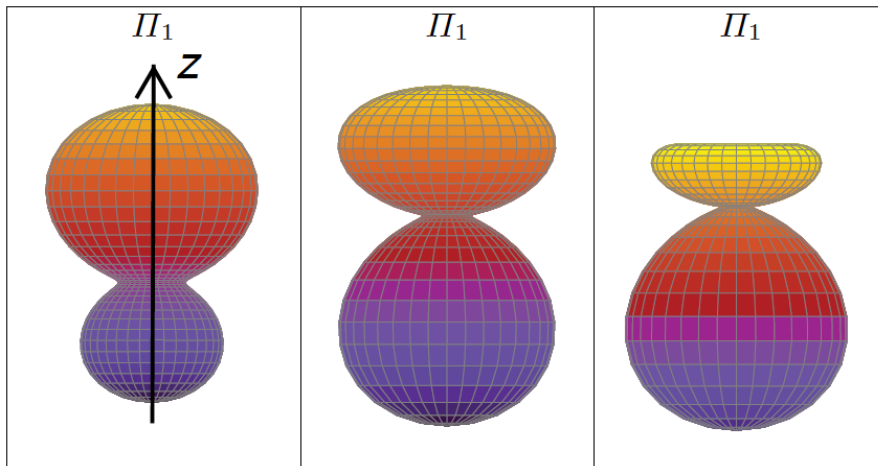
Theoretical Predictions

- We consider pulses of the form $E(t) = F(t) [\cos \omega t + \eta \cos(2\omega t + \phi)]$ with sine-squared pulse envelope $F(t)$ and fundamental peak intensity $I = 10^{12} \text{ W/cm}^2$.

Partial-wave ionization probability



3D PAD



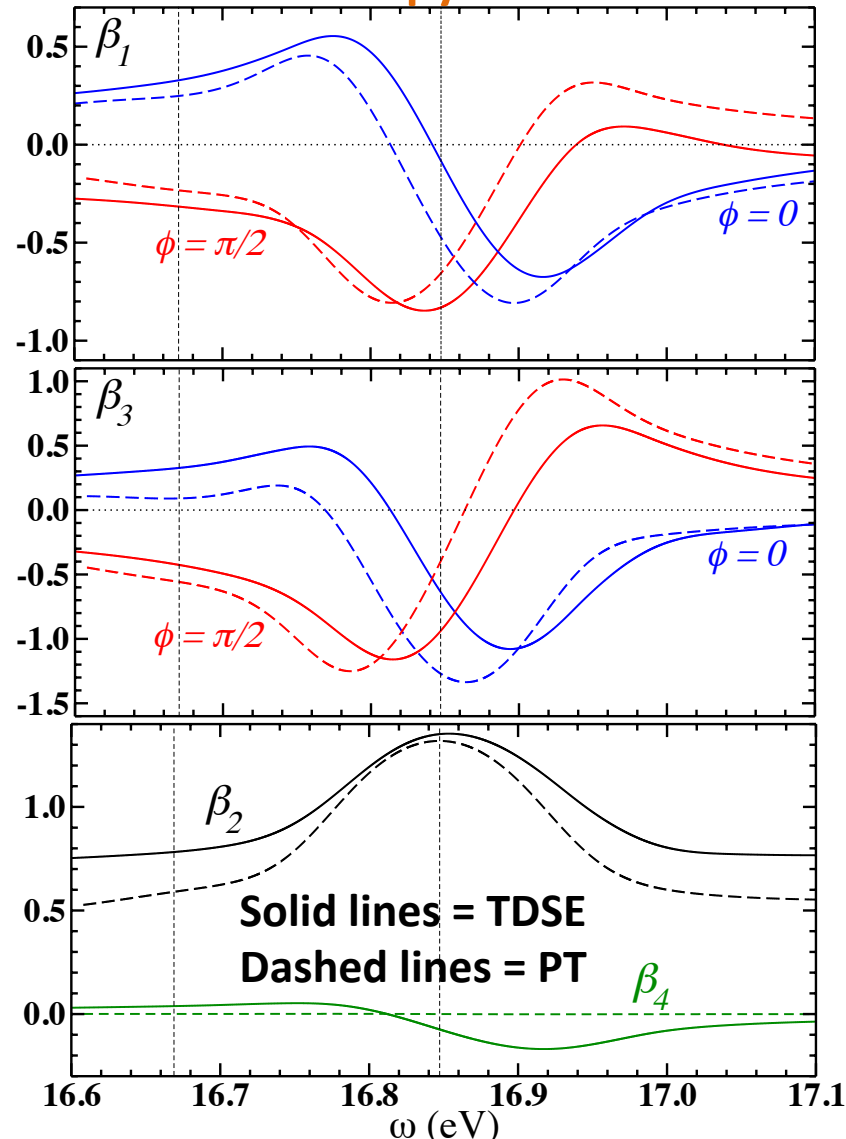
$\omega = 16.81 \text{ eV}$

$\omega = 16.85 \text{ eV}$

$\omega = 16.88 \text{ eV}$

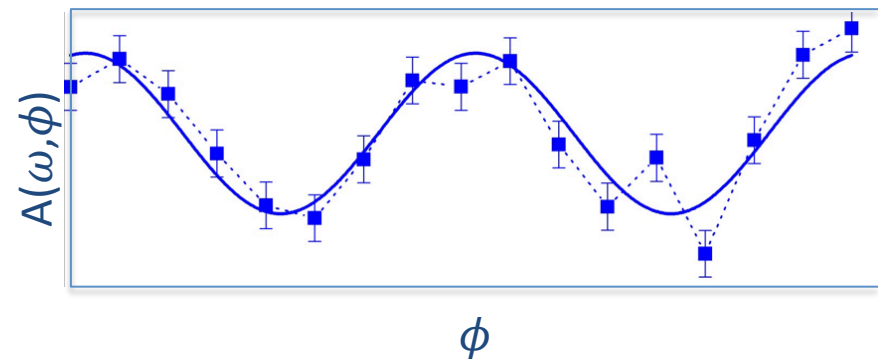
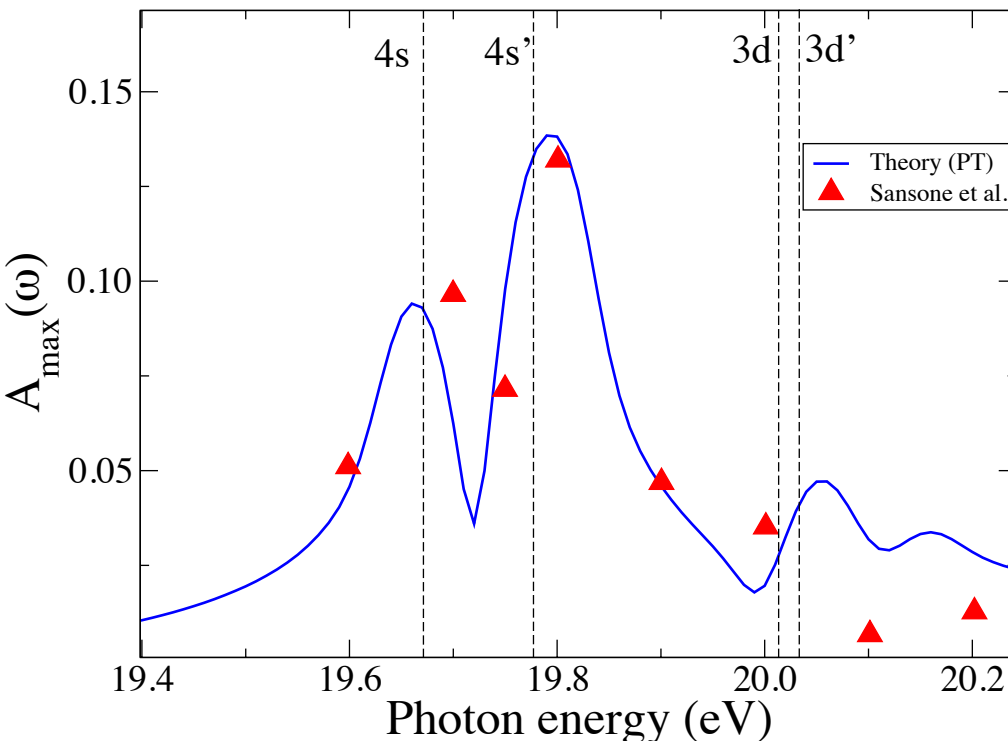
N. Douguet *et al.*, EPJD **72** (2017) 105

Anisotropy Parameters



Using $2p^54s$ as Intermediate States

- Experimentally, the two ($2p^54s$) $J=1$ states were used as intermediate states. This complicates the situation due to:
 - 1) Strong mixture of triplet and singlet in the $4s$ and $4s'$ states.
 - 2) Presence of the $3d$ state in the vicinity and close-lying to the continuum.
- The maximum amplitude and associated phase of the asymmetry were determined by fitting the data to $A(\omega, \phi) = A_{\max}(\omega) \cos(\phi - \phi_{\max}(\omega))$



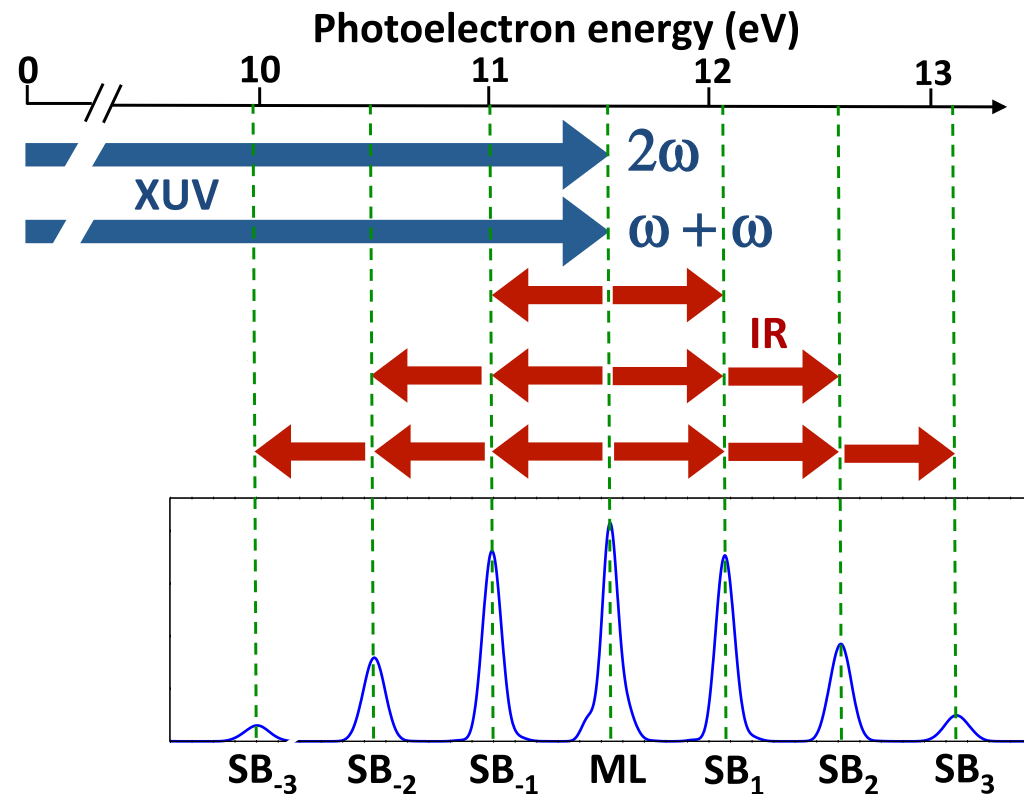
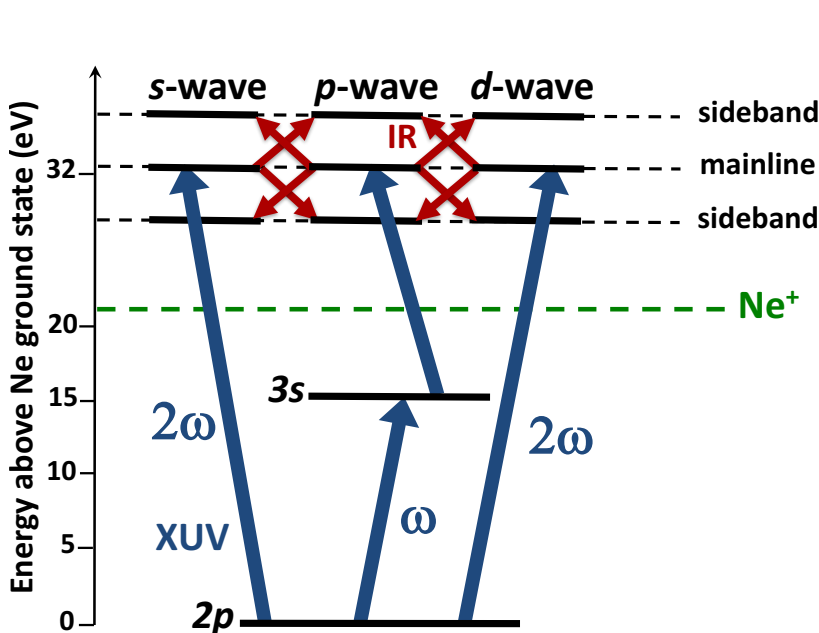
E. Gryzlova *et al.*, in preparation (2017)
G. Sansone *et al.*, "private communication"

Overlapping XUV + IR fields

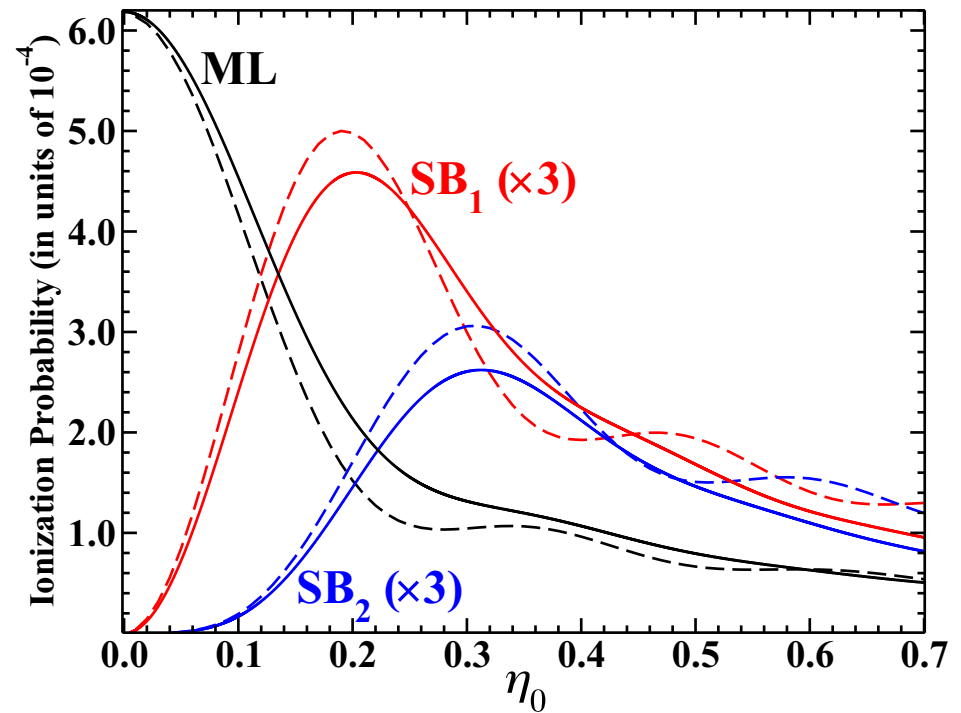
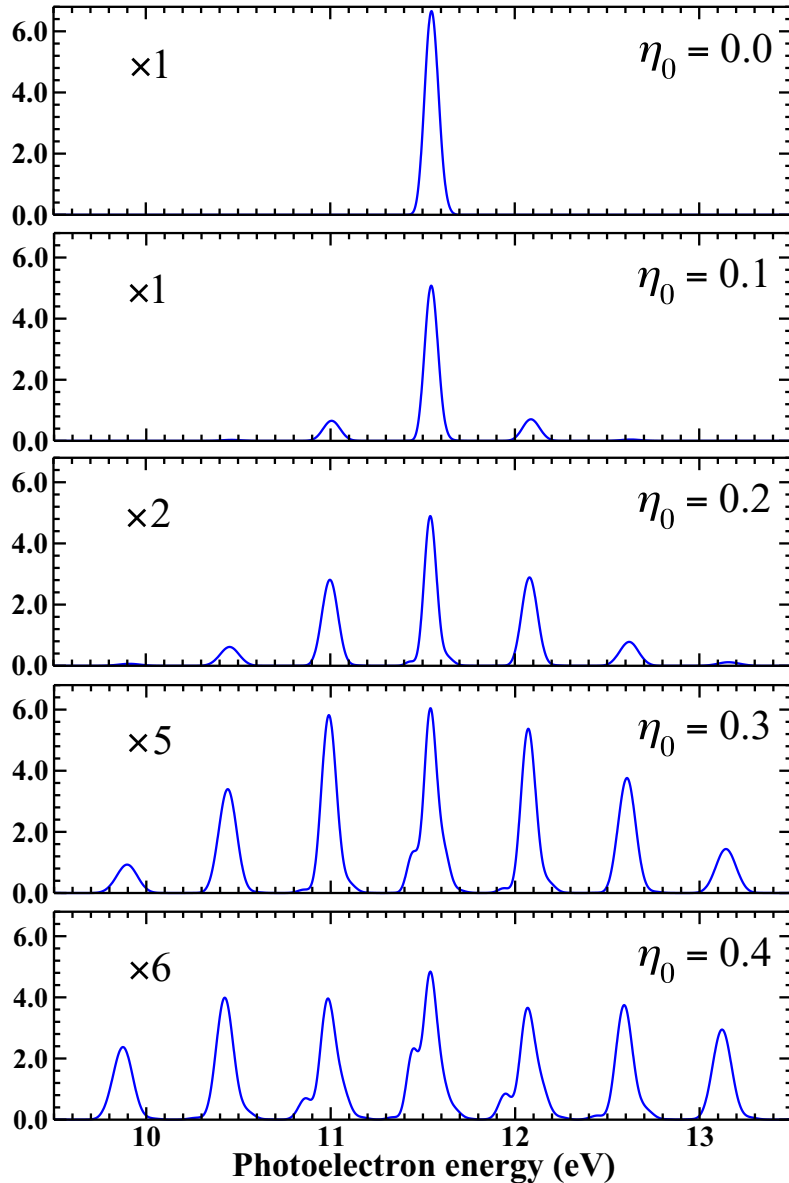
- Can we gain additional control in neon ionization by adding an **infrared field**?

$$\mathcal{E}(t) = \mathcal{E}_X(t) + \mathcal{E}_{IR}(t) \quad \mathcal{E}_X(t) = \bar{\mathcal{E}}_X f(t) [\cos(\omega t) + \eta_X \cos(2\omega t + \varphi_X)]$$

$$\mathcal{E}_{IR}(t) = \eta_0 \bar{\mathcal{E}}_X f(t) \cos(\Omega_0 t + \varphi_0)$$

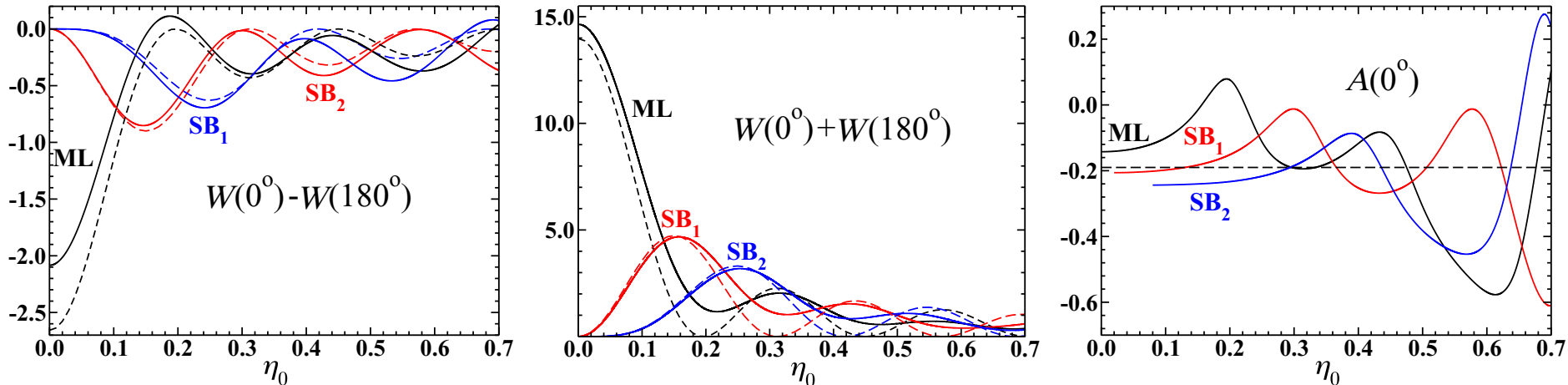


Ionization at the Sidebands



Solid lines = TDSE
Dashed lines = SFA

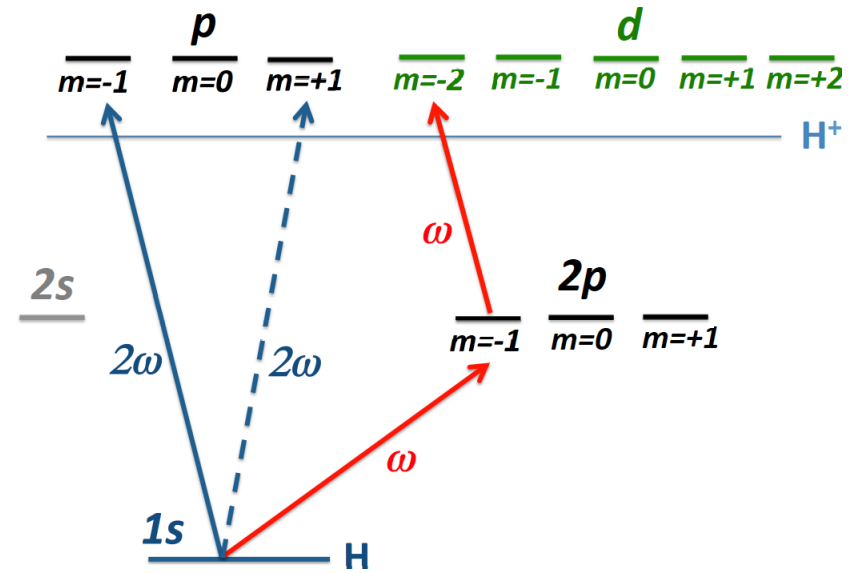
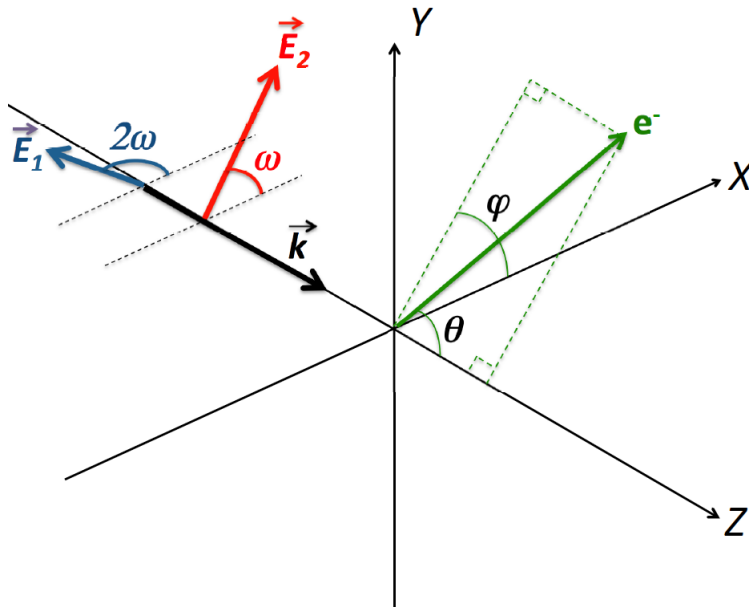
Asymmetry



- The SFA predicts an **asymmetry independent of the IR intensity** for a monochromatic pulse (about -0.2 in this case). Because the infrared field executes many symmetric oscillations, the asymmetry is simply **carried over from one sideband to another in the SFA model**.
- This is clearly not the case in the TDSE prediction.
- We also showed that if the IR frequency **is tuned to a nearby transition** (e.g., $3s \rightarrow 3p$ in neon) then the asymmetry **can be manipulated through the IR frequency and intensity**.

Photoionization Scheme with Circularly Polarized Light in Atomic Hydrogen

- The electric field is in the XY plane and propagates along the Z axis.



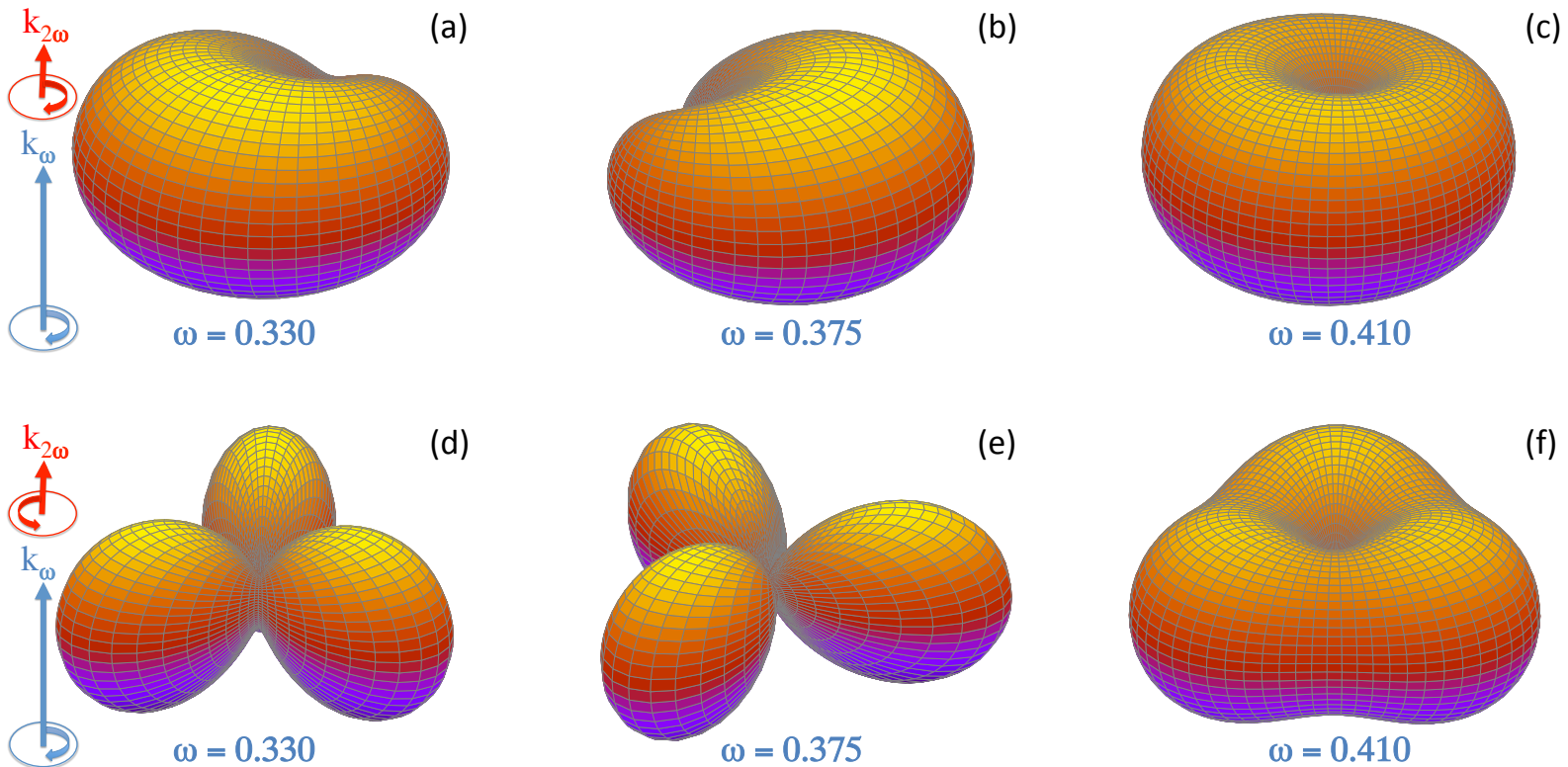
Pulse envelope Amplitude ratio CEP Helicity

$$\mathcal{E}(t) = F(t) \left[\underbrace{\cos(\omega t)\hat{x} - \sin(\omega t)\hat{y}}_{\text{First Harmonic}} + \eta \left\{ \underbrace{\cos(2\omega t + \phi)\hat{x} + \mathcal{H} \sin(2\omega t + \phi)\hat{y}}_{\text{Second Harmonic}} \right\} \right]$$

Electric field

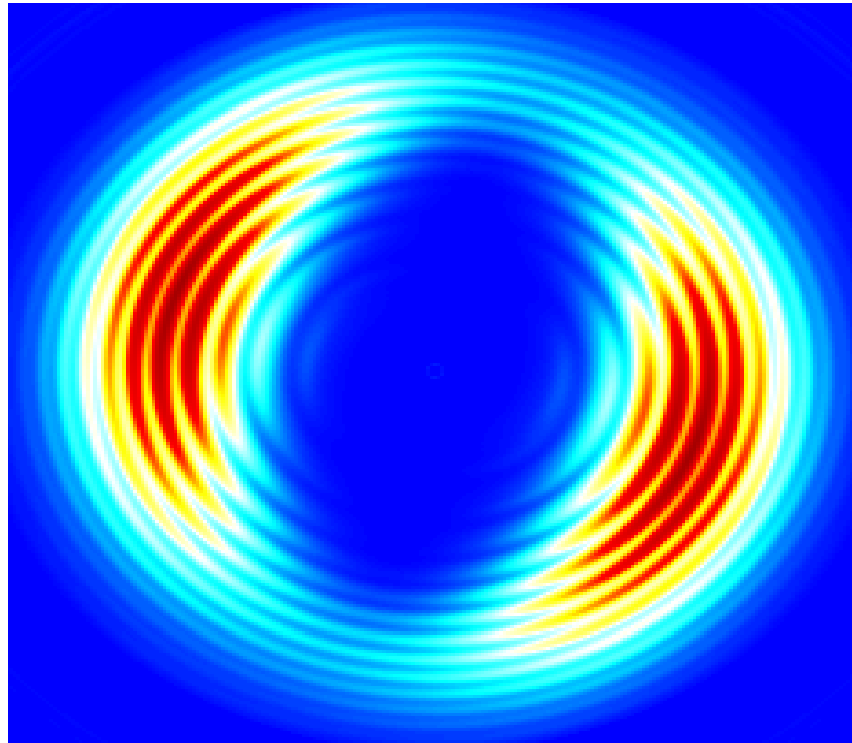
Visualizing the PAD in 3D

$$I = 10^{14} \text{ W/cm}^2$$



N. Douguet *et al.* Phys. Rev. A **93**, 033402 (2016)

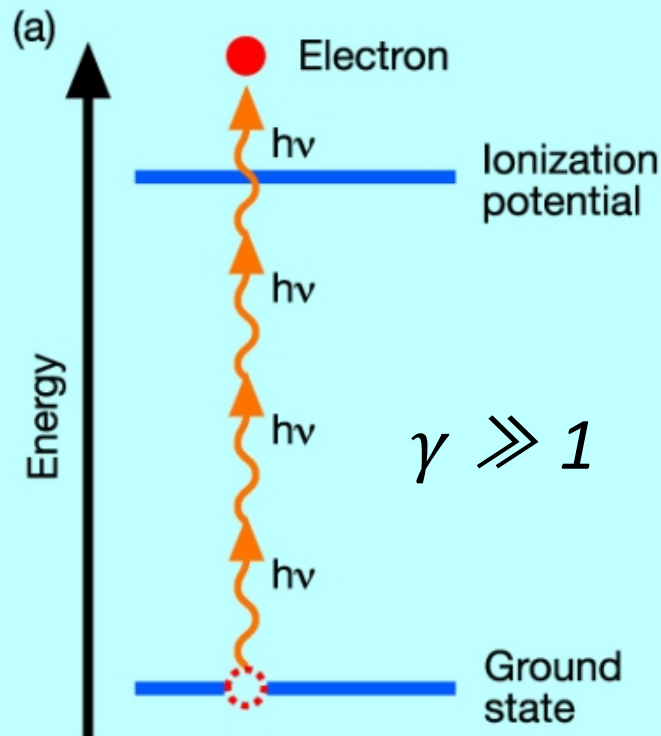
Multiphoton and Tunneling Ionization



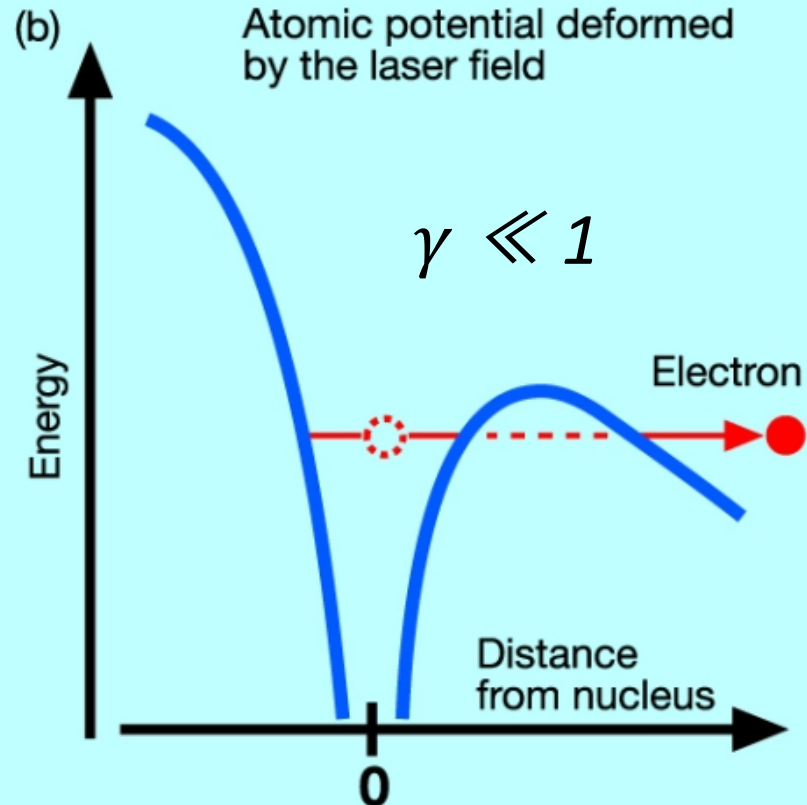
Multiphoton and Tunneling Ionization

- The Keldysh parameter $\gamma = (I_p/2U_p)^{1/2}$, with I_p the ionization potential and U_p the ponderomotive energy.

Multiphoton Ionization

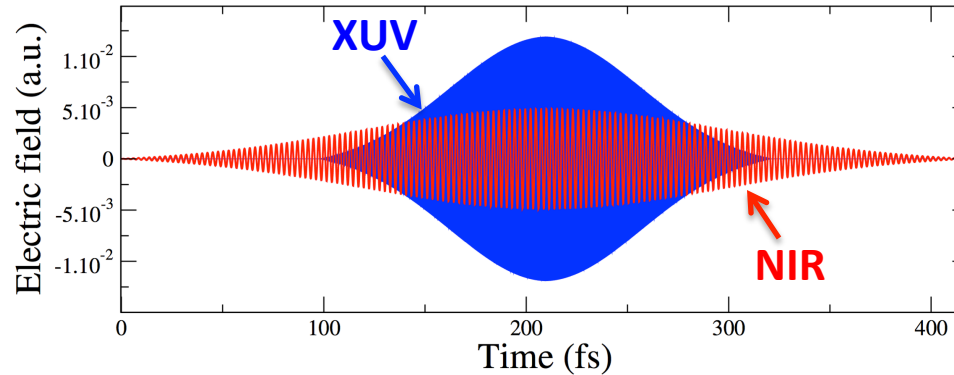


Tunneling Ionization



Circular Dichroism in Oriented He^+

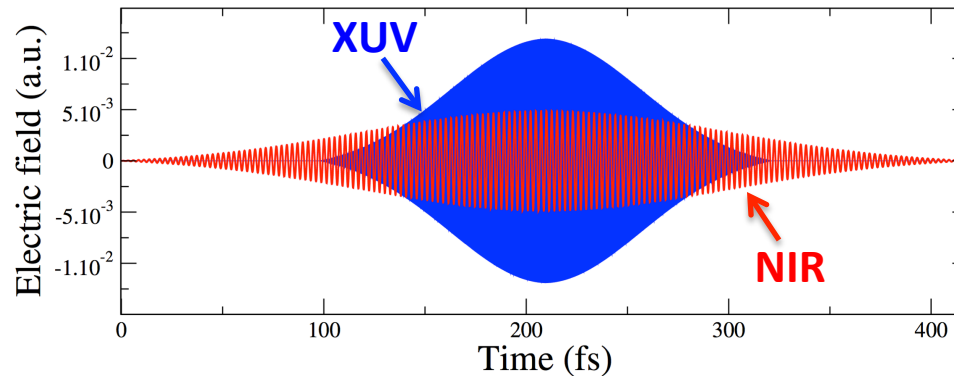
- An overlapping circular XUV + NIR field is created at the FEL at FERMI



- The circularly polarized XUV pulse (FWHM = 100 fs and $I = 10^{13} \text{ W/cm}^2$ with positive helicity ($\mathcal{H} = +1$) creates oriented $\text{He}^+(3p ; m = +1)$ via sequential absorption of two XUV photons:

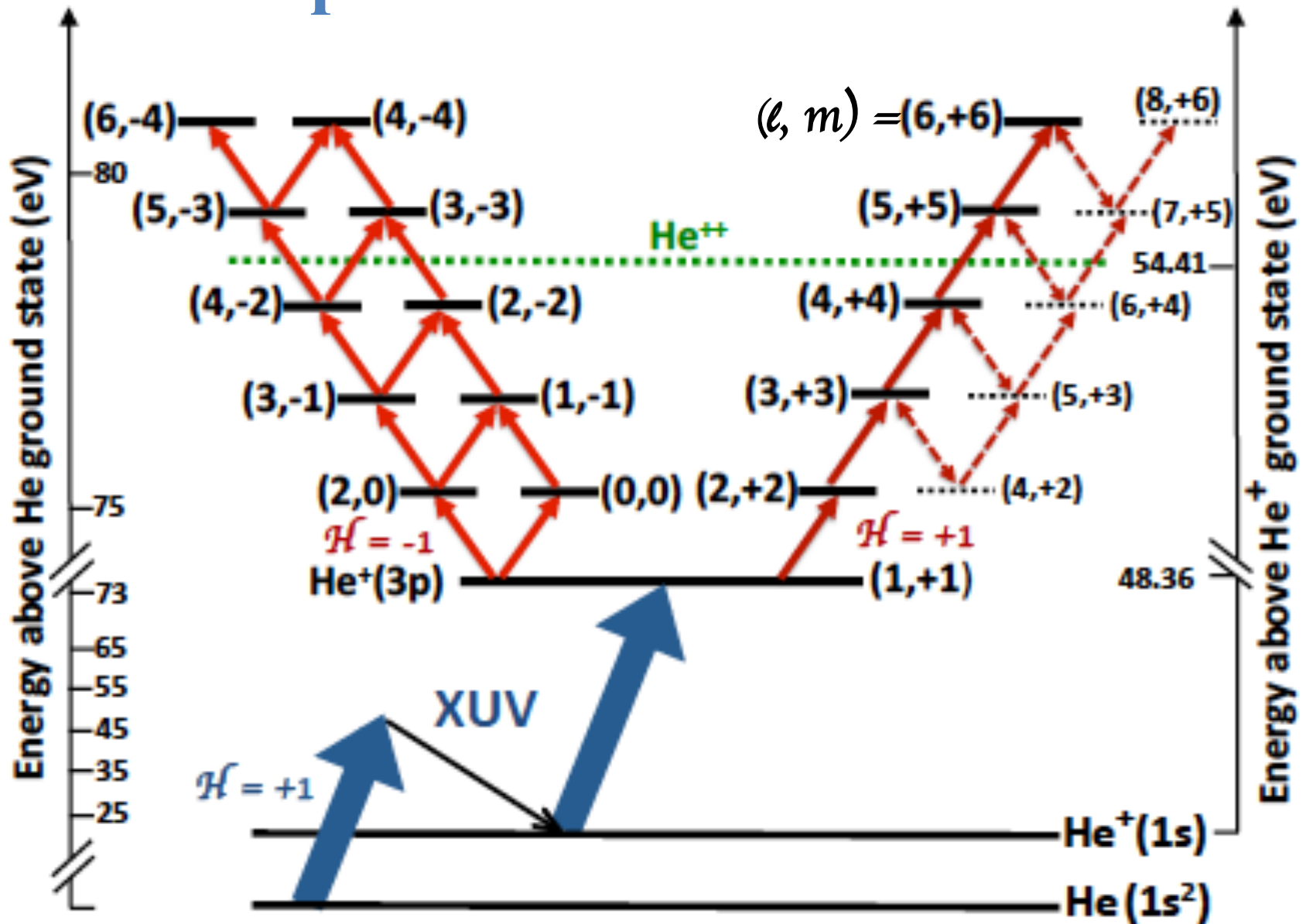
Circular Dichroism in Oriented He^+

- An overlapping circular XUV + NIR field is created at the FEL at FERMI

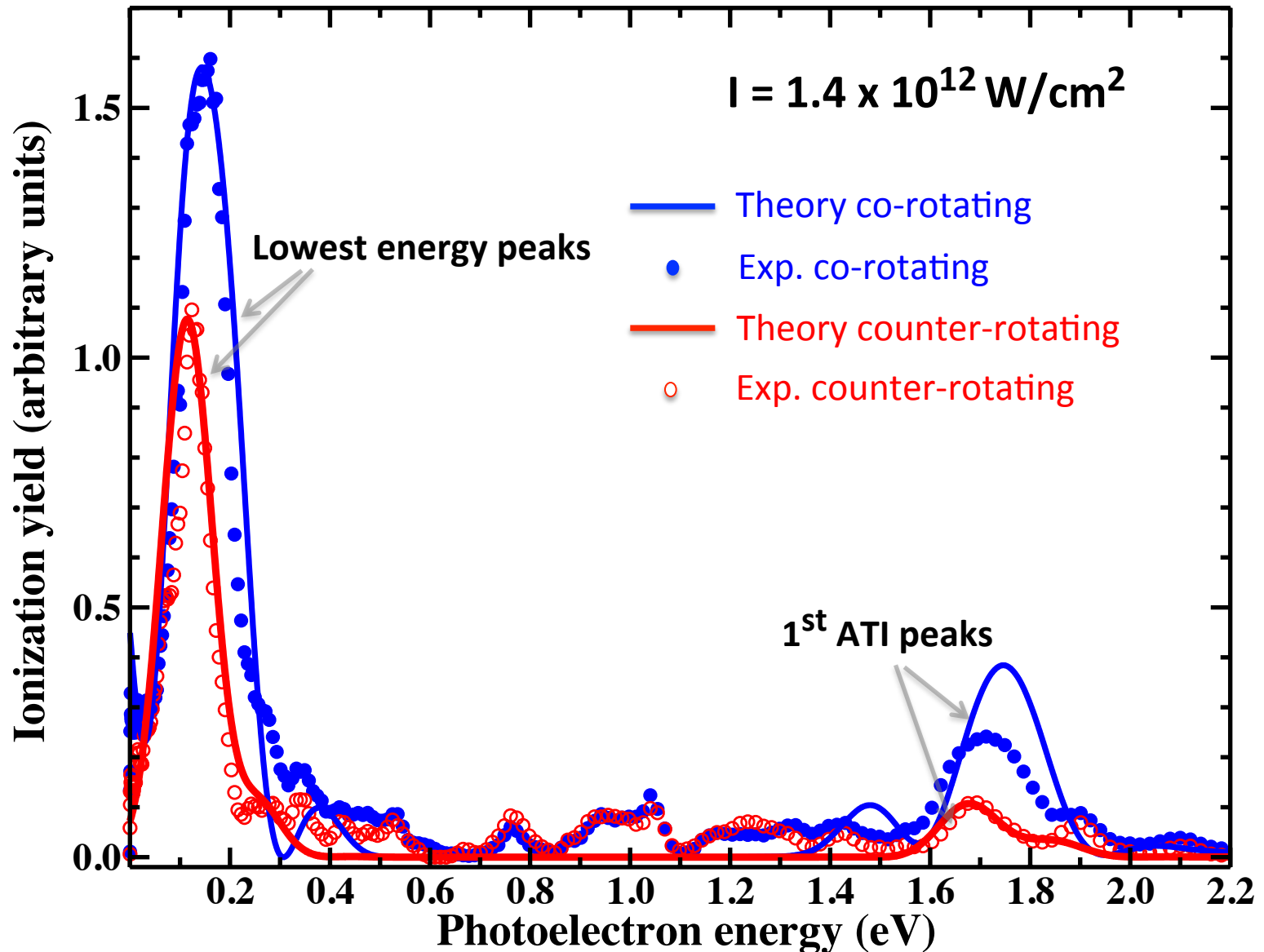


- The circularly polarized XUV pulse (FWHM = 100 fs and $I = 10^{13} \text{ W/cm}^2$ with positive helicity ($\mathcal{H} = +1$) creates oriented $\text{He}^+(3p; m = +1)$ via sequential absorption of two XUV photons:
 - Ionization**: $\text{He}(1s^2) + h\nu (48.37 \text{ eV}) \rightarrow \text{He}^+(1s) + e^-$
 - Pumping**: $\text{He}^+(1s) + h\nu (48.37 \text{ eV}) \rightarrow \text{He}^+(3p; m = +1)$
- The overlapping circularly polarized optical laser pulse (FWHM = 170 fs) with ($\mathcal{H} = +1$) or ($\mathcal{H} = -1$) ionizes the oriented $\text{He}^+(3p; m = +1)$ ion.
 - Multiphoton ionization**: $\text{He}^+(3p; m = +1) + 4 h\nu (1.58 \text{ eV}) \rightarrow \text{He}^{++} + e^-$

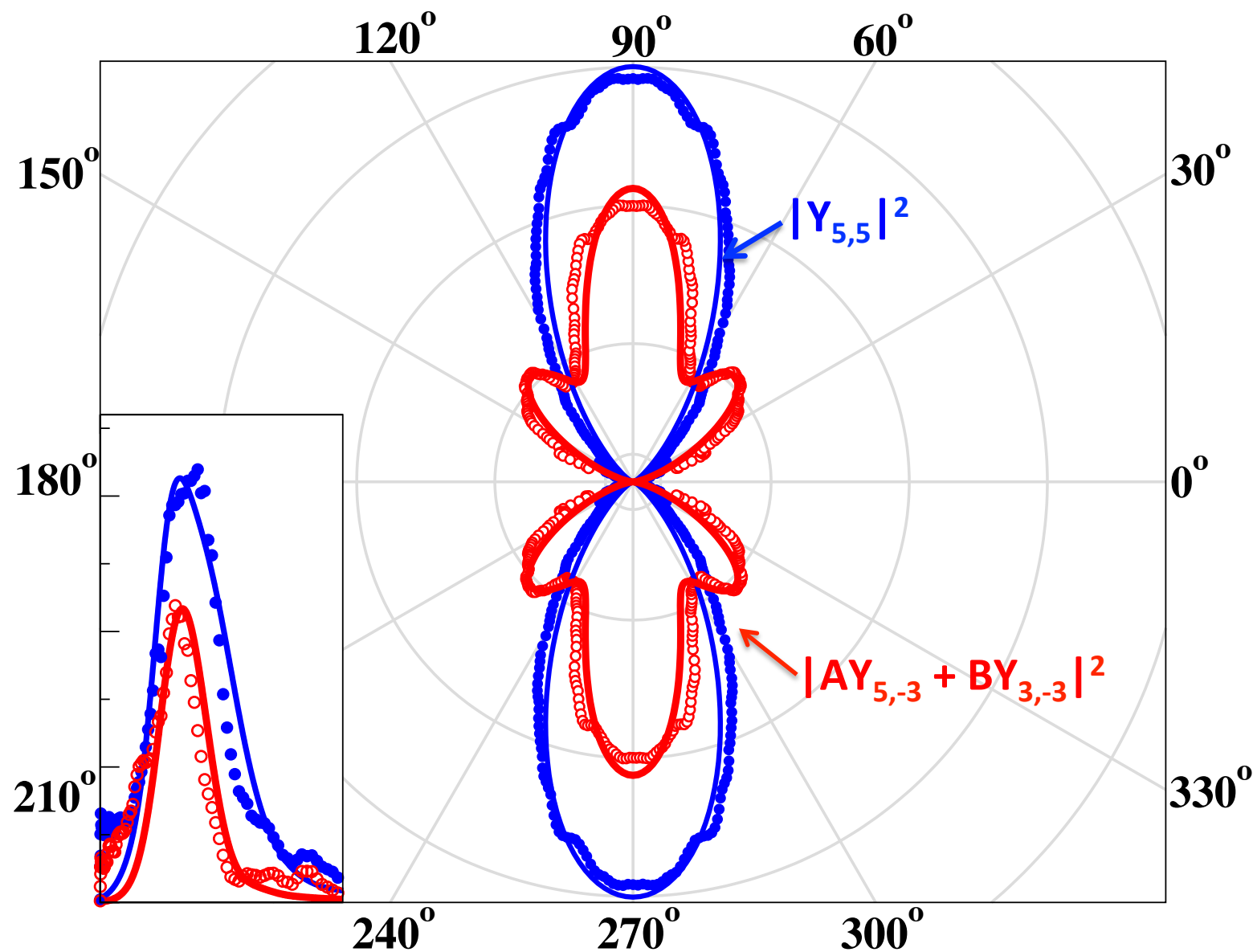
Multiphoton ionization scheme



Photoelectron spectrum



Photoelectron angular distribution



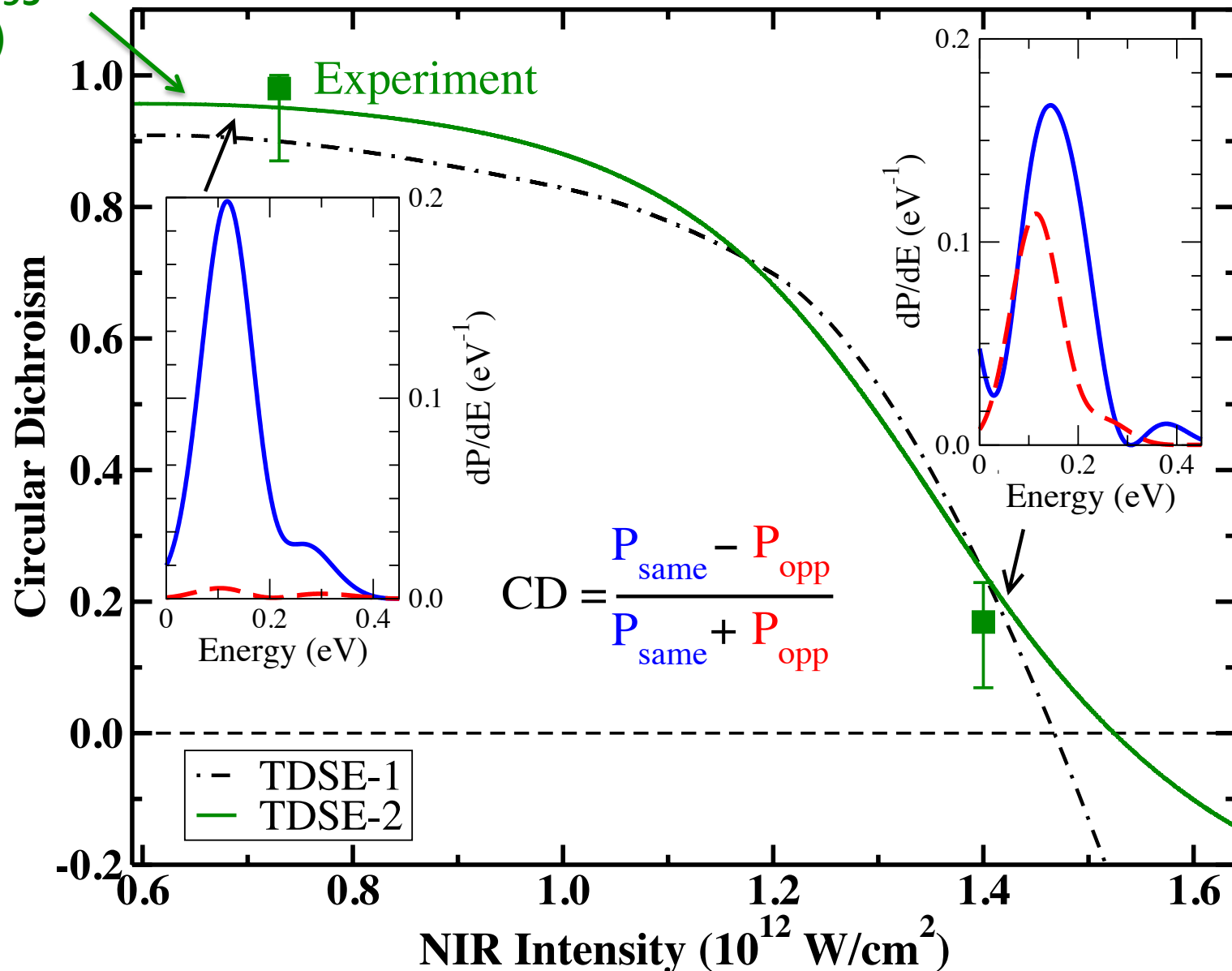
M. Ilchen, N. Douguet *et al.*, Phys. Rev. Lett. **118**, 013002 (2017)

Intensity dependence

- The photoionization spectrum was studied as a function of the **optical field intensity** from $I = 5 \times 10^{11} \text{ W/cm}^2$ to about $I = 2 \times 10^{12} \text{ W/cm}^2$.
- The ionization at the lowest peak was measured/calculated for both co-rotating and counter-rotating field helicities. **The circular dichroism** is defined as $\text{CD} = [\mathbf{P}_{\text{same}} - \mathbf{P}_{\text{opp}}] / [\mathbf{P}_{\text{same}} + \mathbf{P}_{\text{opp}}]$.

Circular Dichroism

CD ≈ 0.95
(LOPT)



Intensity dependence

- The photoionization spectrum was studied as a function of the **optical field intensity** from $I = 5 \times 10^{11} \text{ W/cm}^2$ to about $I = 2 \times 10^{12} \text{ W/cm}^2$.
- The ionization at the lowest peak was measured/calculated for both co-rotating and counter-rotating field helicities. **The circular dichroism** is defined as $\text{CD} = [P_{\text{same}} - P_{\text{opp}}] / [P_{\text{same}} + P_{\text{opp}}]$.
- From LOPT, the ionization probability for co-rotating fields is expected **to be much larger** than for counter-rotating fields **at low intensity** since the angular factor is about **50 times larger** for the same field helicity.
- A negative CD was predicted by Barth and Smirnova [**PRA 84 0634153 (2011)**] in the tunneling ionization regime.

Intensity dependence

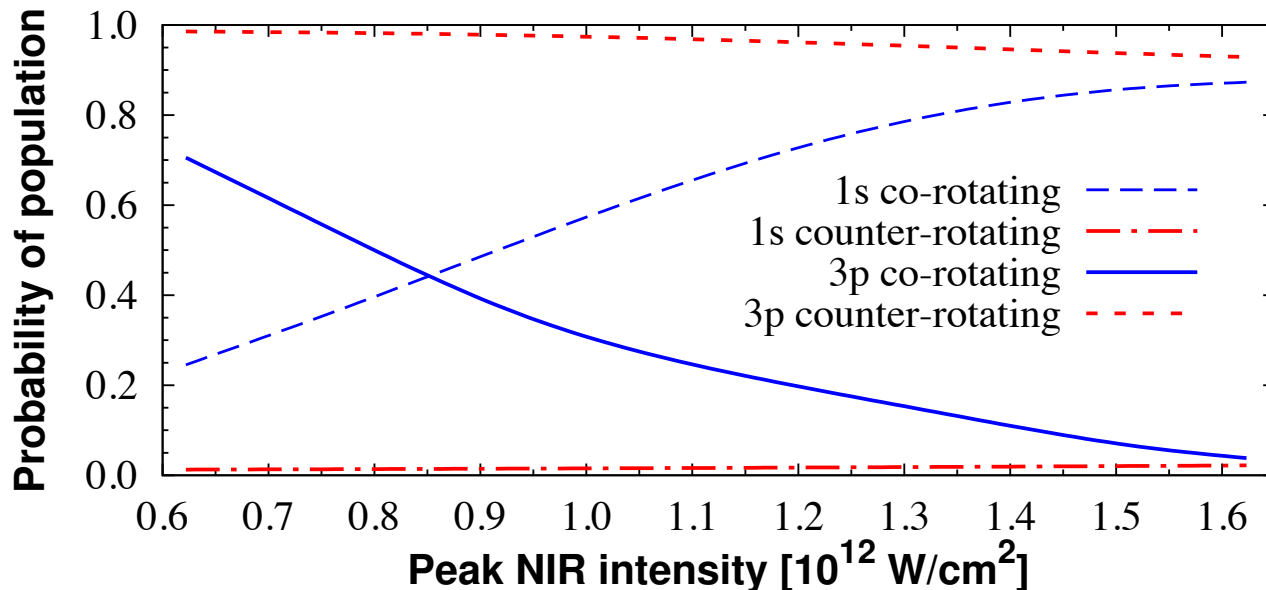
- The photoionization spectrum was studied as a function of the **optical field intensity** from $I = 5 \times 10^{11} \text{ W/cm}^2$ to about $I = 2 \times 10^{12} \text{ W/cm}^2$.
- The ionization at the lowest peak was measured/calculated for both co-rotating and counter-rotating field helicities. **The circular dichroism** is defined as **$CD = [P_{\text{same}} - P_{\text{opp}}] / [P_{\text{same}} + P_{\text{opp}}]$** .
- From LOPT, the ionization probability for co-rotating fields is expected **to be much larger** than for counter-rotating fields **at low intensity** since the angular factor is about **50 times larger** for the same field helicity.
- A negative CD was predicted by Barth and Smirnova [**PRA 84 0634153 (2011)**] in the tunneling ionization regime.
- However, as the intensity is only slightly increased, the **CD decreases rapidly** and is predicted to become **negative** at only $I = 1.55 \times 10^{12} \text{ W/cm}^2$!

Intensity Dependence

- The photoionization spectrum was studied as a function of the **optical field intensity** from $I = 5 \times 10^{11} \text{ W/cm}^2$ to about $I = 2 \times 10^{12} \text{ W/cm}^2$.
- The ionization at the lowest peak was measured/calculated for both co-rotating and counter-rotating field helicities. **The circular dichroism** is defined as $\text{CD} = [P_{\text{same}} - P_{\text{opp}}] / [P_{\text{same}} + P_{\text{opp}}]$.
- From LOPT, the ionization probability for co-rotating fields is expected **to be way larger** than for counter-rotating fields **at low intensity**
→ The angular factor is about 50 times larger for the same field helicity!
- A negative CD was predicted by Barth and Smirnova [**PRA 84 0634153 (2011)**] in the tunneling ionization regime.
- However, as the intensity is only slightly increased, the **CD decreases rapidly** and is predicted to become **negative** at only $1.55 \times 10^{12} \text{ W/cm}^2$!
→ **Why do we observe a negative CD at low field intensity!?**

Discussion

- The behavior of the CD is most probably the result of several factors.
- Our analysis strongly suggests that two important factors play a role:
 - i. Changing the optical frequency strongly modifies the CD
→ Suggests **near-resonant** phenomena
 - ii. The **AC stark shift** of the 3p state is larger in the co-rotating case than in the counter-rotating case (confirmed by Fourier-analysis).
→ 3p state is not efficiently populated for co-rotating fields.



Counter-rotating

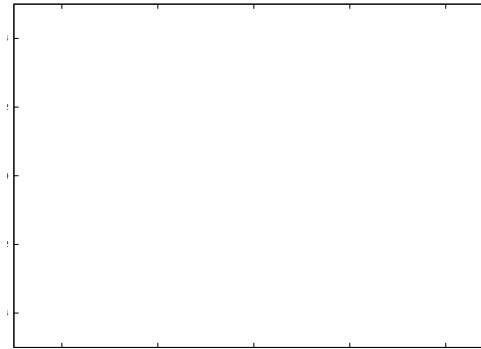
3p, m= +1

AC stark shift

Co-rotating

Illustration: Dichroism at $I = 10^{12} \text{ W/cm}^2$

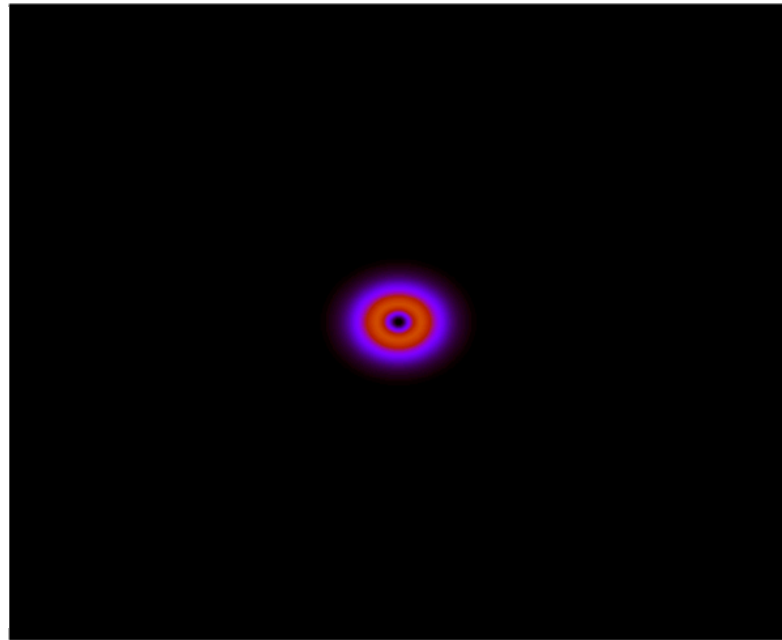
Pulse : 4 cycles and $\lambda = 780 \text{ nm}$
Target: Hydrogen $2p(+1)$ state.



$$\gamma = 11.1$$

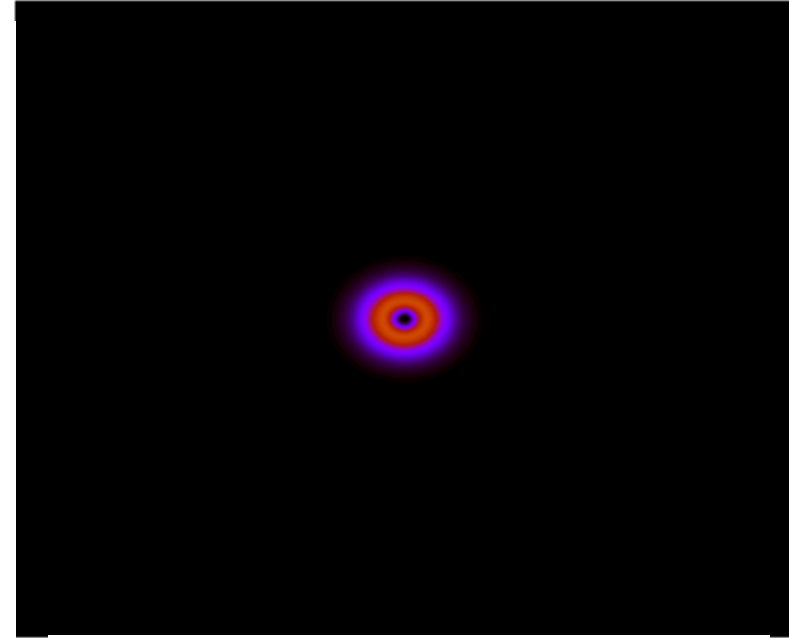


Co-rotating
($m = +1$)



Ionization Probability = 6.532×10^{-2}

Counter-rotating
($m = -1$)

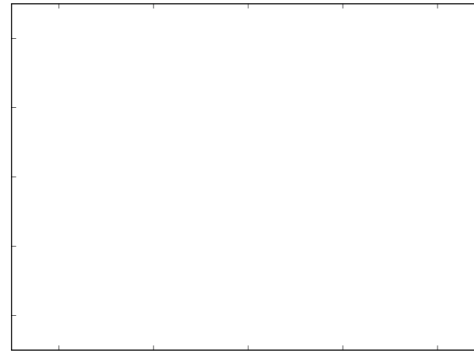


Ionization Probability = 1.572×10^{-2}

Illustration: Dichroism at $I = 10^{12} \text{ W/cm}^2$

Pulse : 4 cycles and $\lambda = 780 \text{ nm}$
Target: Hydrogen 2p state.

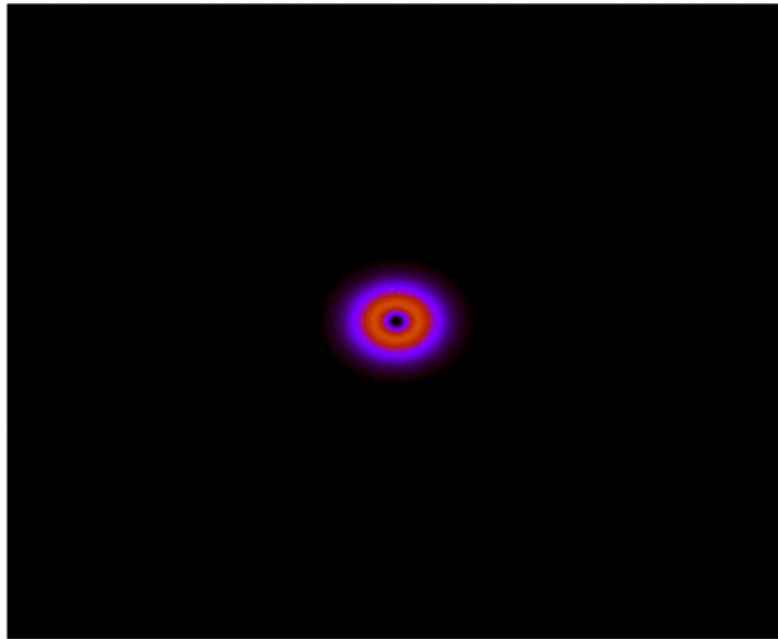
$$\gamma = 11.1$$



$$F = -eE(t)$$

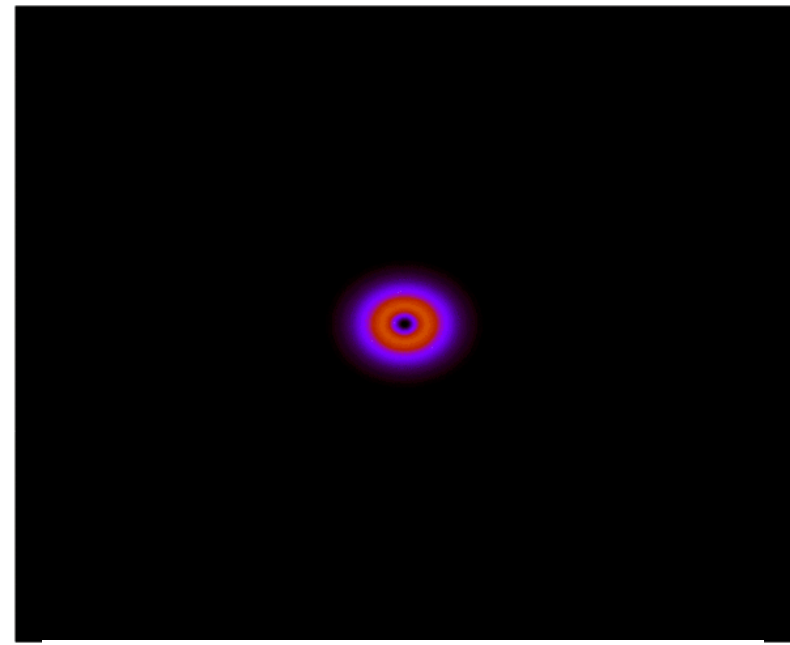


Co-rotating
($m = +1$)



Ionization Probability = 6.532×10^{-2}

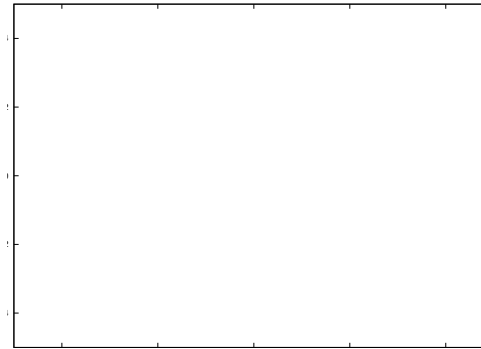
Counter-rotating
($m = -1$)



Ionization Probability = 1.572×10^{-2}

Illustration: Dichroism at $I = 4 \times 10^{13} \text{ W/cm}^2$

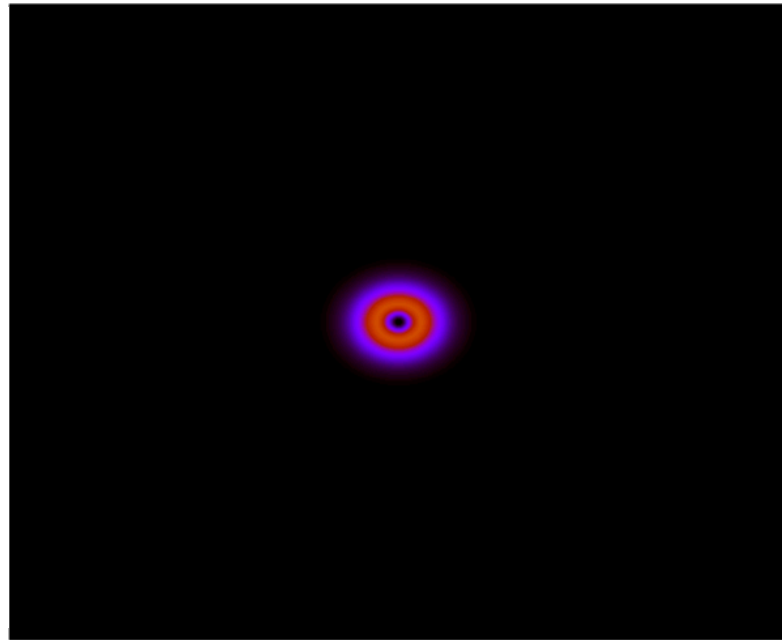
Pulse : 4 cycles and $\lambda = 780 \text{ nm}$
Target: Hydrogen 2p state.



$$\gamma = 1.75$$

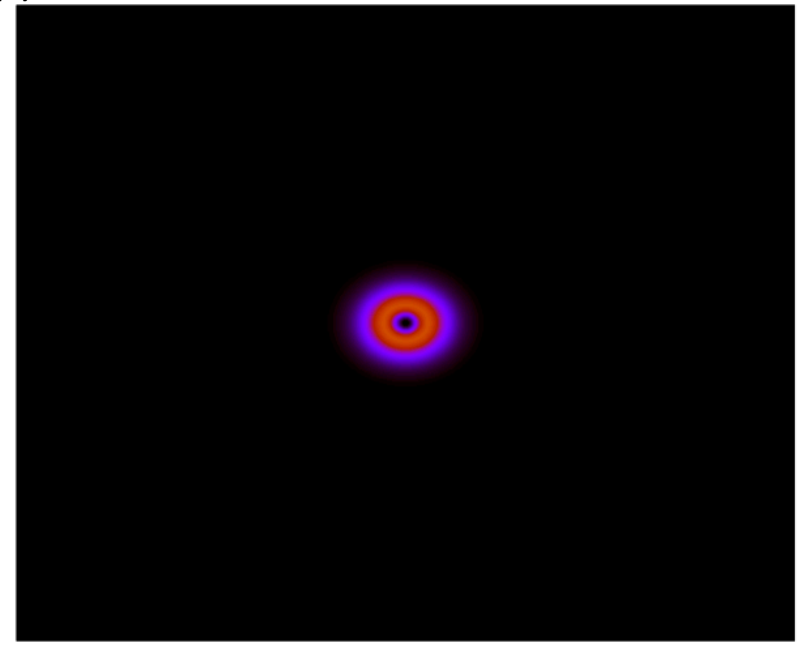


Co-rotating
($m = +1$)



Ionization Probability = $7.01\text{e-}01$

Counter-rotating
($m = -1$)

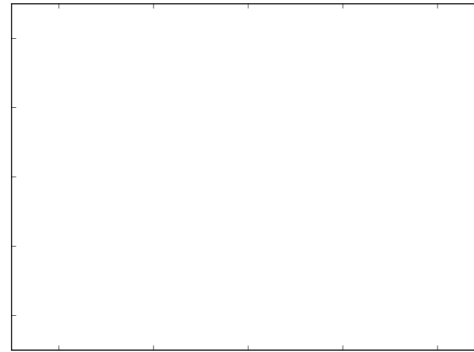


Ionization Probability = $7.72\text{e-}01$

Illustration: Dichroism at $I = 4 \times 10^{13} \text{ W/cm}^2$

Pulse : 4 cycles and $\lambda = 780 \text{ nm}$
Target: Hydrogen 2p state

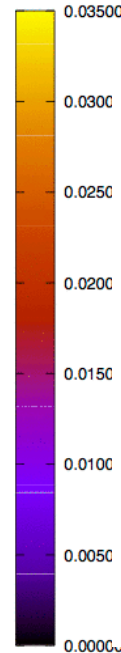
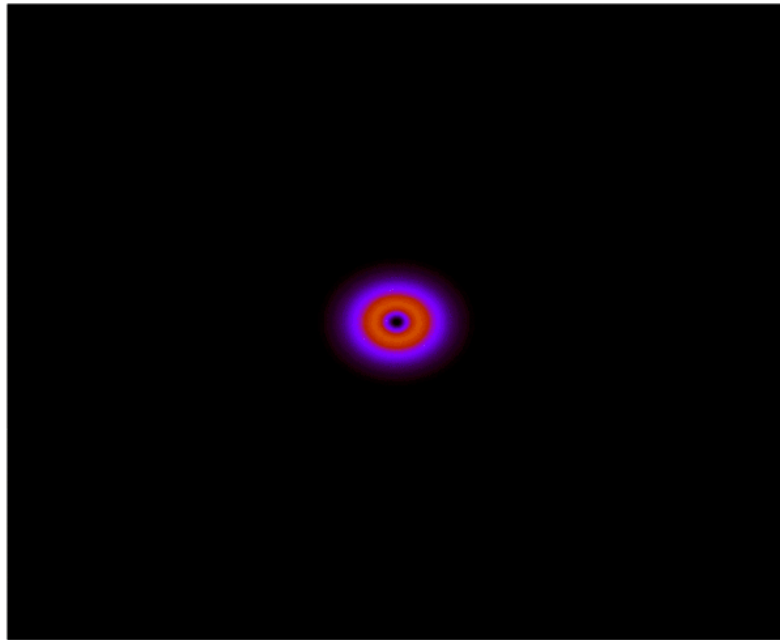
$$\gamma = 1.75$$



$$F = -eE(t)$$

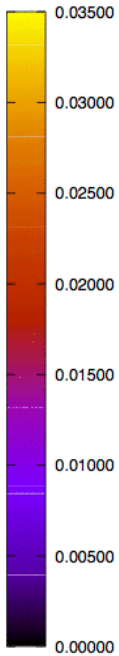
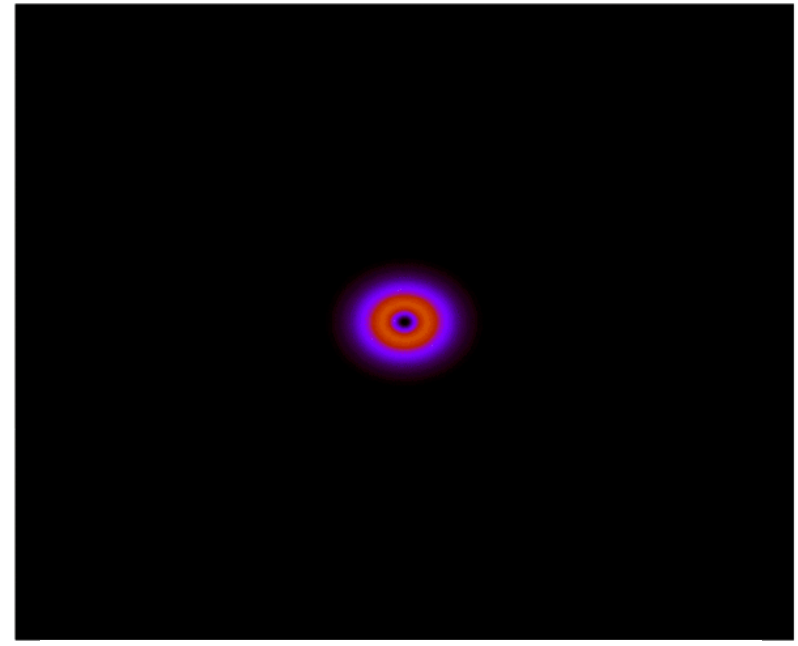


Co-rotating
($m = +1$)



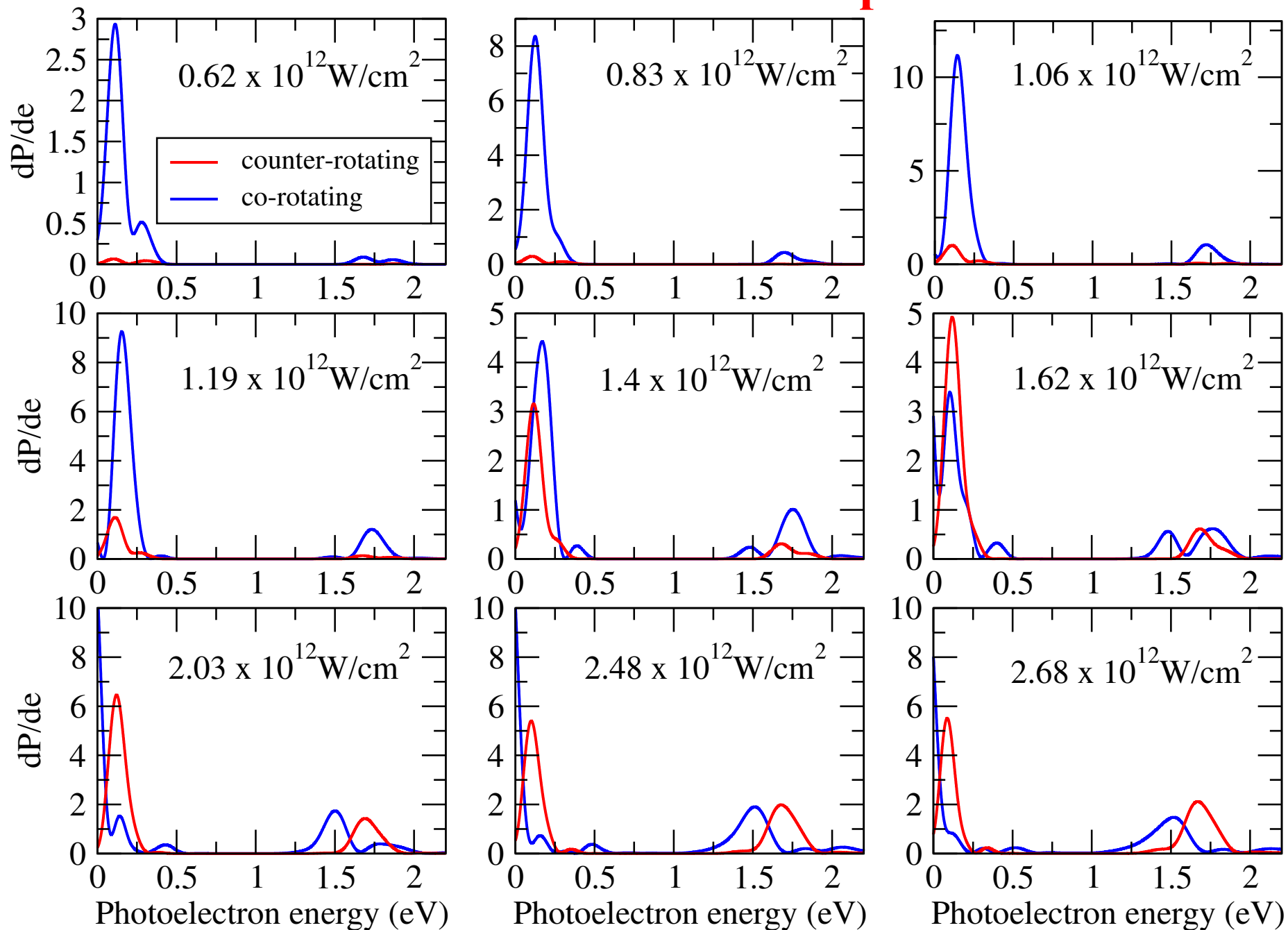
Ionization Probability = $7.01\text{e-}01$

Counter-rotating
($m = -1$)

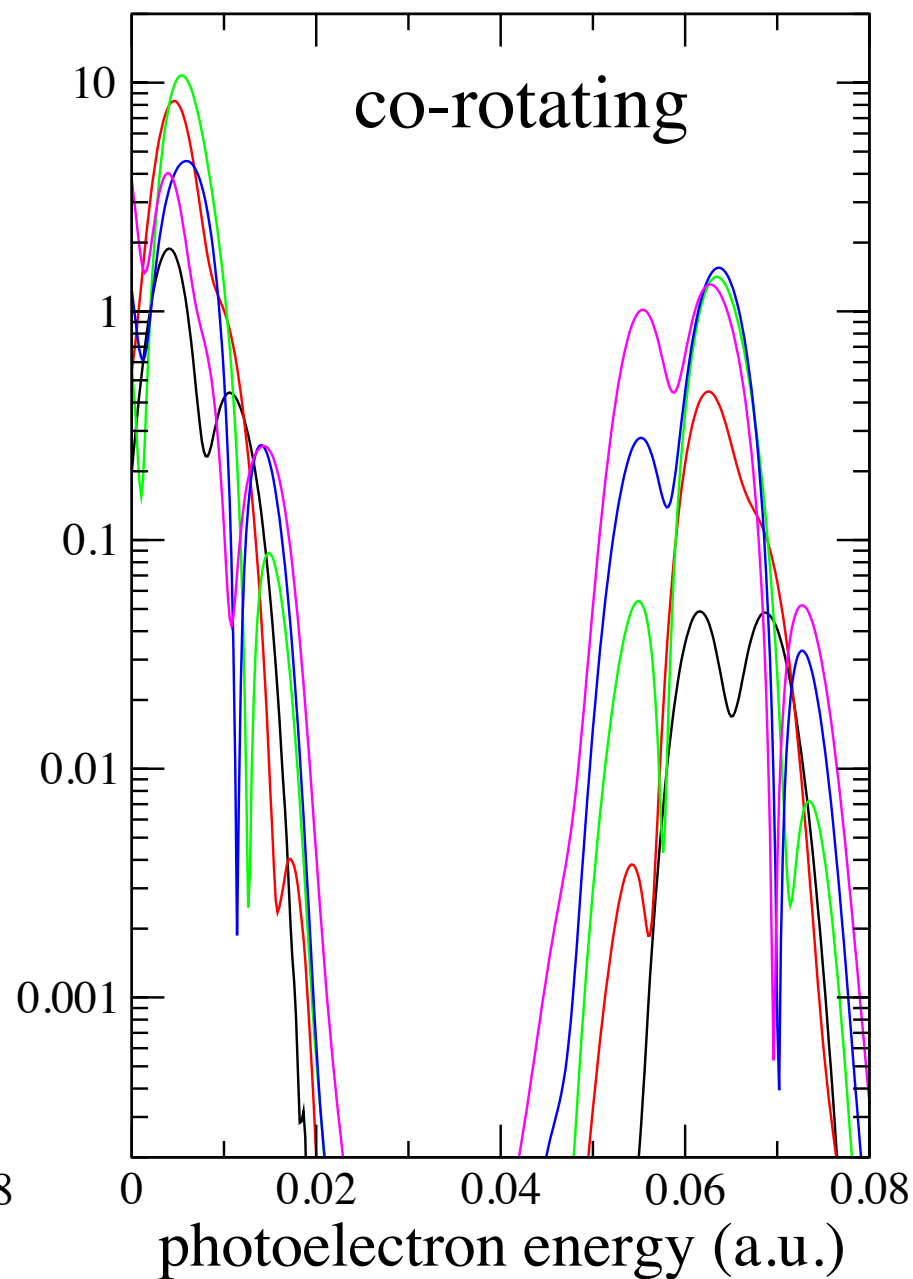
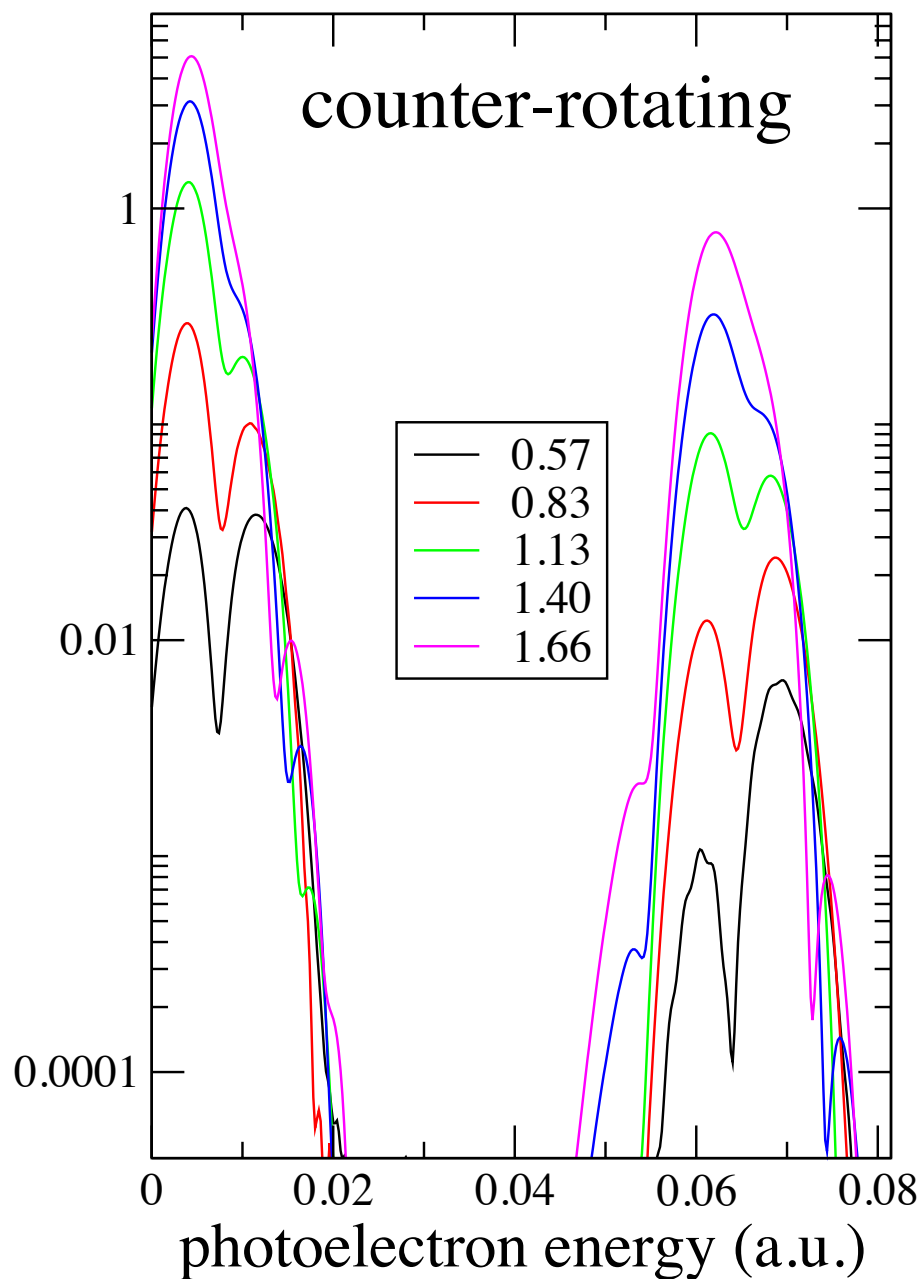


Ionization Probability = $7.72\text{e-}01$

Overview for a number of IR peak intensities



It's pretty complicated: 3-peak structure with strong IR dependence



Tunneling Time

(a somewhat controversial topic)

nature
physics

ARTICLES

PUBLISHED ONLINE: 25 MAY 2015 | DOI: 10.1038/NPHYS3340

Interpreting attoclock measurements of tunnelling times

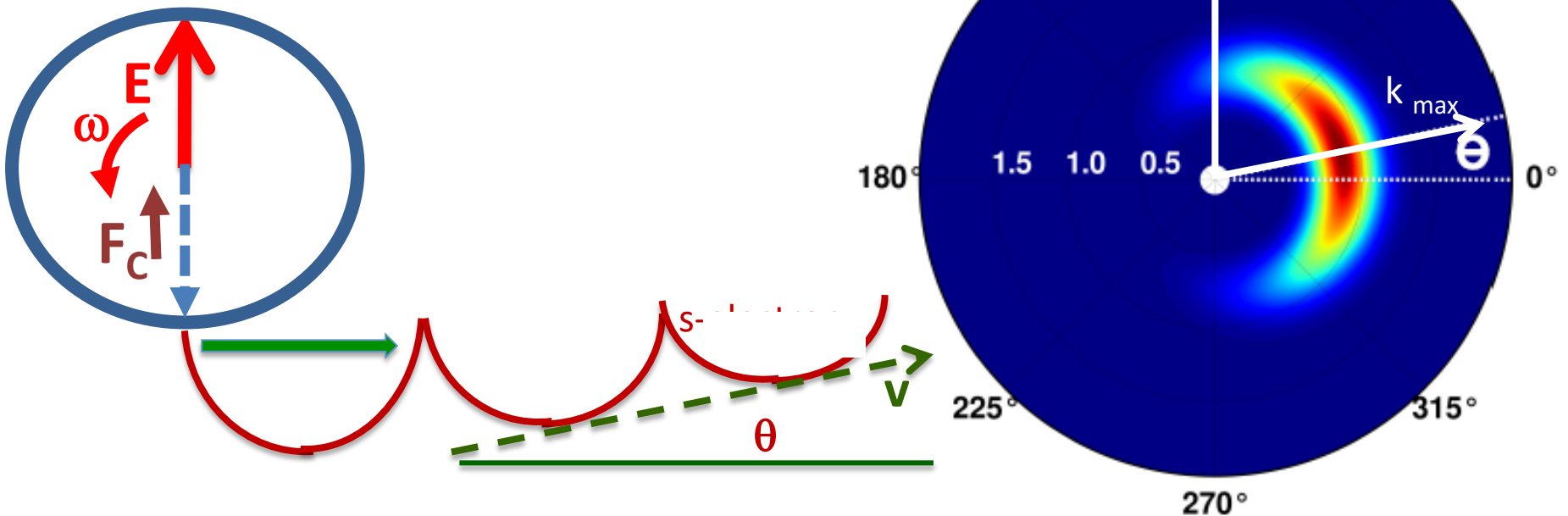
Lisa Torlina^{1†}, Felipe Morales^{1†}, Jivesh Kaushal¹, Igor Ivanov², Anatoli Kheifets², Alejandro Zielinski³, Armin Scrinzi³, Harm Geert Muller¹, Suren Sukiasyan⁴, Misha Ivanov^{1,4,5} and Olga Smirnova^{1★}

Resolving in time the dynamics of light absorption by atoms and molecules, and the electronic rearrangement this induces, is among the most challenging goals of attosecond spectroscopy. The attoclock is an elegant approach to this problem, which encodes ionization times in the strong-field regime. However, the accurate reconstruction of these times from experimental data presents a formidable theoretical task. Here, we solve this problem by combining analytical theory with *ab initio* numerical simulations. We apply our theory to numerical attoclock experiments on the hydrogen atom to extract ionization time delays and analyse their nature. Strong-field ionization is often viewed as optical tunnelling through the barrier created by the field and the core potential. **We show that, in the hydrogen atom, optical tunnelling is instantaneous.** We also show how calibrating the attoclock using the hydrogen atom opens the way to identifying possible delays associated with multielectron dynamics during strong-field ionization.

Tunneling Time (atto-clock?)

TDSE spectra

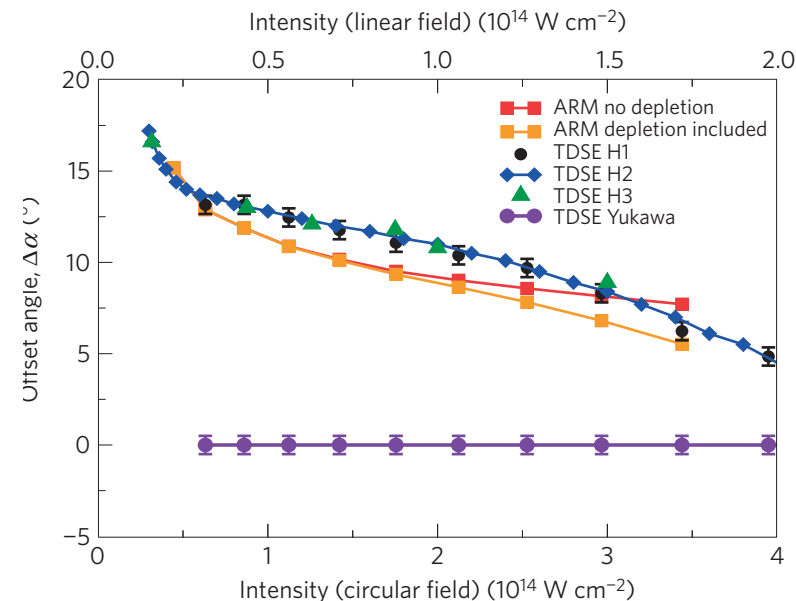
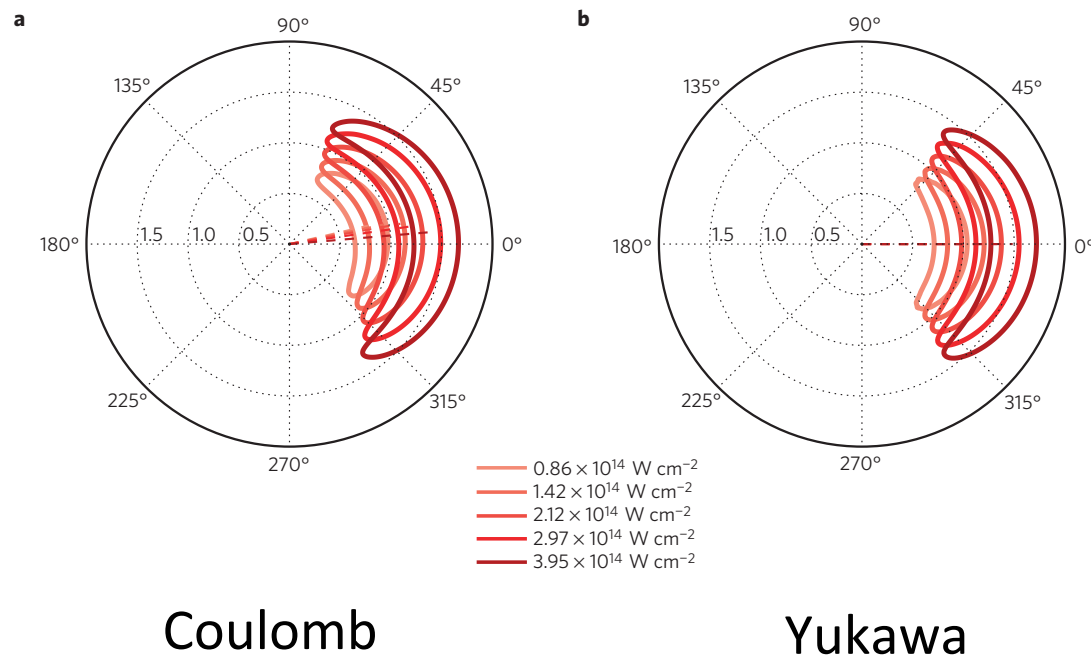
[adapted from Torlina *et al.*,
Nat. Phys. **11** (2016) 593]



- Assumption: Since the probability for tunneling ionization varies exponentially with the field strength, ionization occurs at the maximum of the field. From the offset angle (non-zero due to the long-range Coulomb potential), one hopes to read off the time (atto-clock).

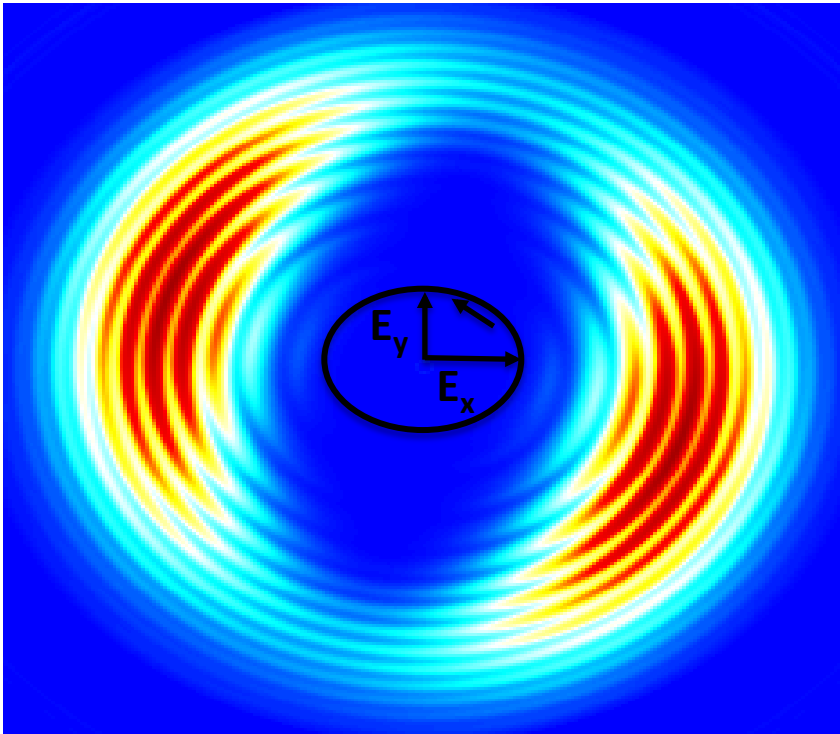
Comparison with Short-Range Potential

- The offset angle can have **two origins**: (i) the effect of the long-range Coulomb potential, and/or (ii) the time it takes for the electron to tunnel through the barrier.
 - In order to answer this question, Torlina *et al.* performed calculations using a short-range **Yukawa potential** with the same energy of the 1s state.
- They found zero offset using the Yukawa potential and concluded that tunneling is **instantaneous** in atomic hydrogen. *Is this a valid conclusion?*

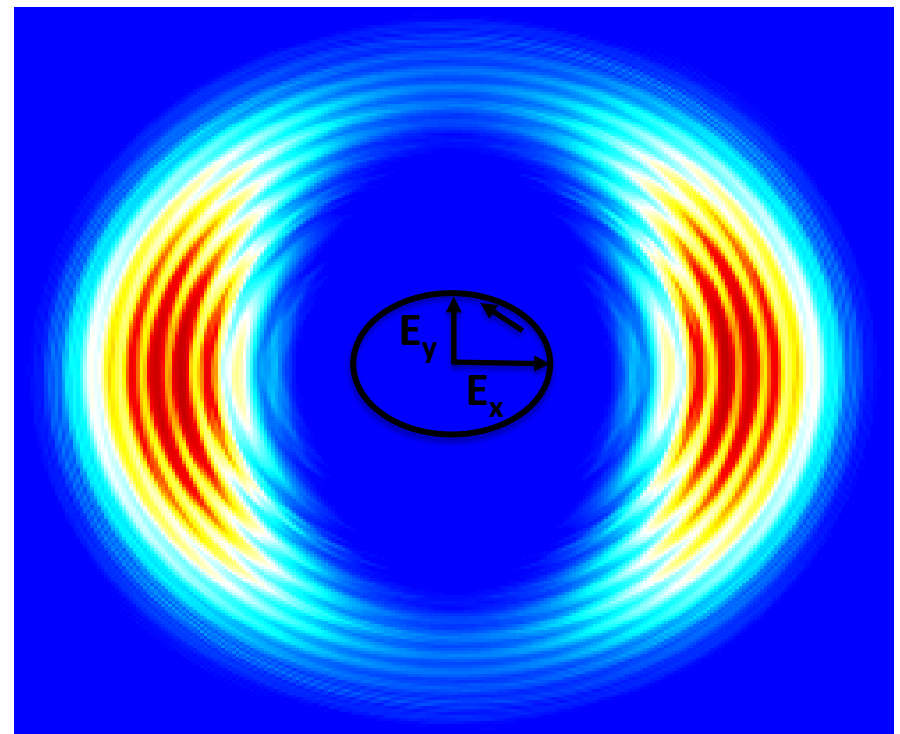


Theoretical Predictions for a Realistic Experiment

- Recently we started collaborating with other theorists to describe a more realistic experiment performed at **Griffith University**. It uses a 6-cycle (FWHM) pulse with wavelength $\lambda = 770$ nm and ellipticity $\varepsilon = 0.84$. The CEP is not controlled and must be averaged over. In the examples below, the peak intensity is 1.4×10^{14} W/cm².



Coulomb

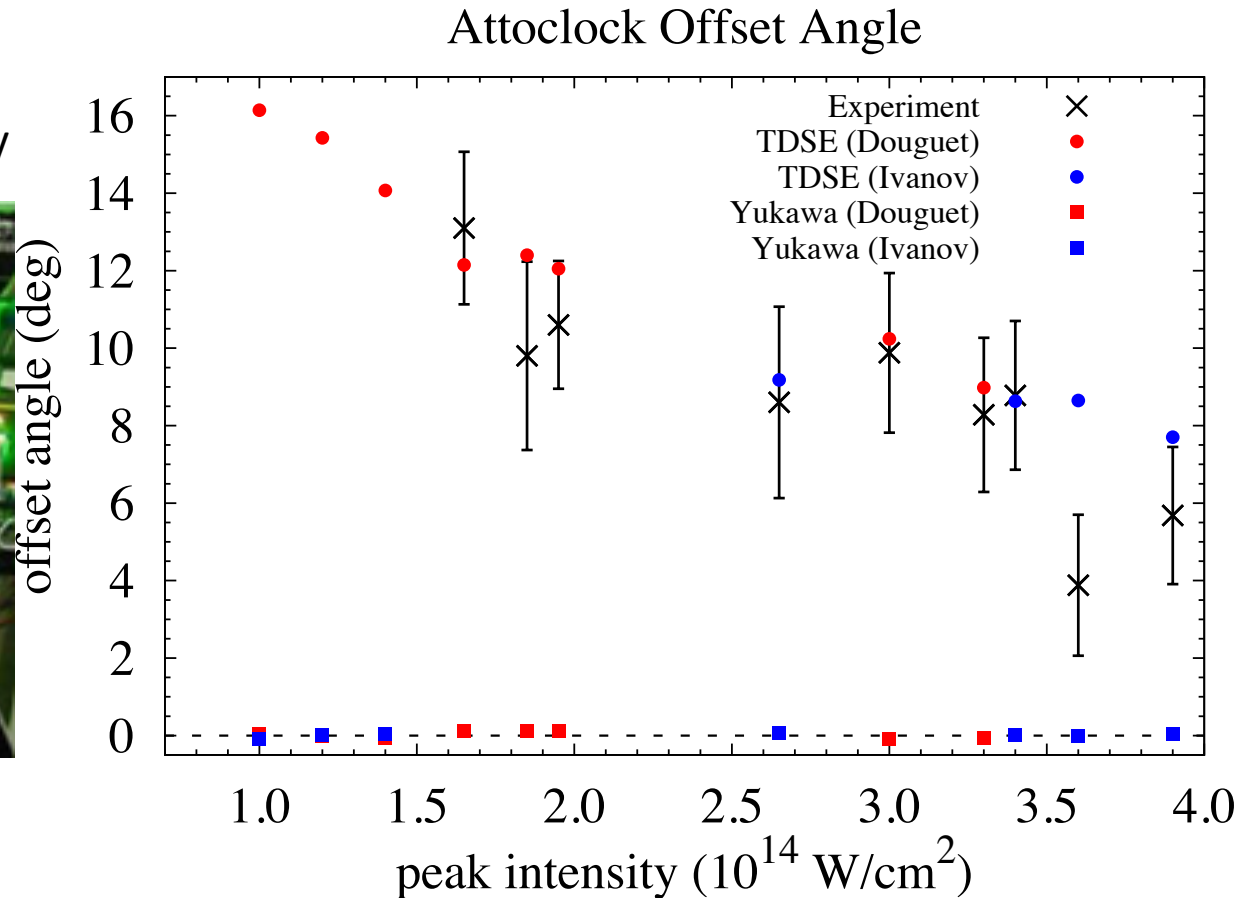
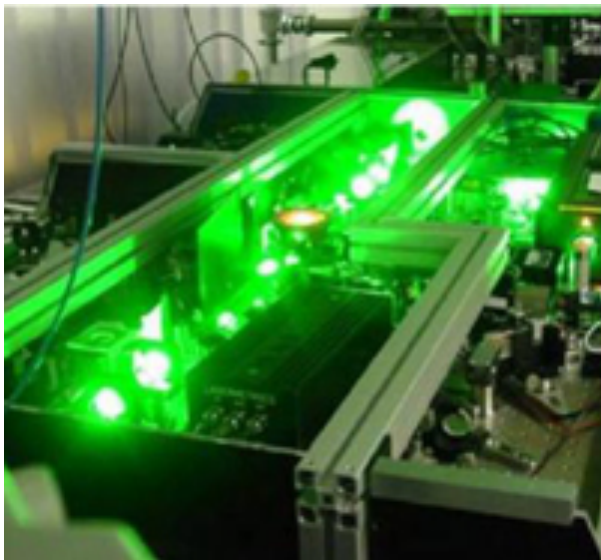


Yukawa

Comparison with Experimental Data

(preliminary results of S. Satya, I. Litvinyuk, ...)

The Australian AttoSecond
Facility at Griffith University



- So far **good agreement** is observed between experiment and theory, which provides confidence in both.
- The results are intended to be used to **calibrate the attoclock** for future studies on more complex systems.

Bohmian Mechanics

- Bohmian Mechanics can be useful in **interpreting results** obtained in a fully quantum mechanical approach.

Bohmian Mechanics

- Bohmian Mechanics can be useful in **interpreting results** obtained in a fully quantum mechanical approach.
- The basic idea (illustrated here in 1D) is the following:

Suppose $\varphi(x, t) = R(x, t) \exp [iS(x, t)]$ is the solution of the TDSE. Then $\rho(x, t) = R(x, t)^2$ is the probability density, $v(x, t)$ is the velocity field, and $V_C(x, t)$ and $V_Q(x, t) = -0.5\Delta R(x, t)/R(x, t)$ are the classical and quantum potentials, respectively.

Bohmian Mechanics

- Bohmian Mechanics can be useful in **interpreting results** obtained in a fully quantum mechanical approach.
- The basic idea (illustrated here in 1D) is the following:

Suppose $\varphi(x, t) = R(x, t) \exp [iS(x, t)]$ is the solution of the TDSE. Then $\rho(x, t) = R(x, t)^2$ is the probability density, $v(x, t)$ is the velocity field, and $V_C(x, t)$ and $V_Q(x, t) = -0.5\Delta R(x, t)/R(x, t)$ are the classical and quantum potentials, respectively.

- The velocity field can be obtained from the flux and charge densities.
- Bohmian trajectories, labeled by their starting point x_0 , are calculated as in Classical Mechanics with $v_0 = 0$.
- The quantum potential allows for motion in the classically forbidden region.

The manuscript is currently being revised ...

Dynamics of Tunneling Ionization using Bohmian Mechanics

Nicolas Douguet and Klaus Bartschat

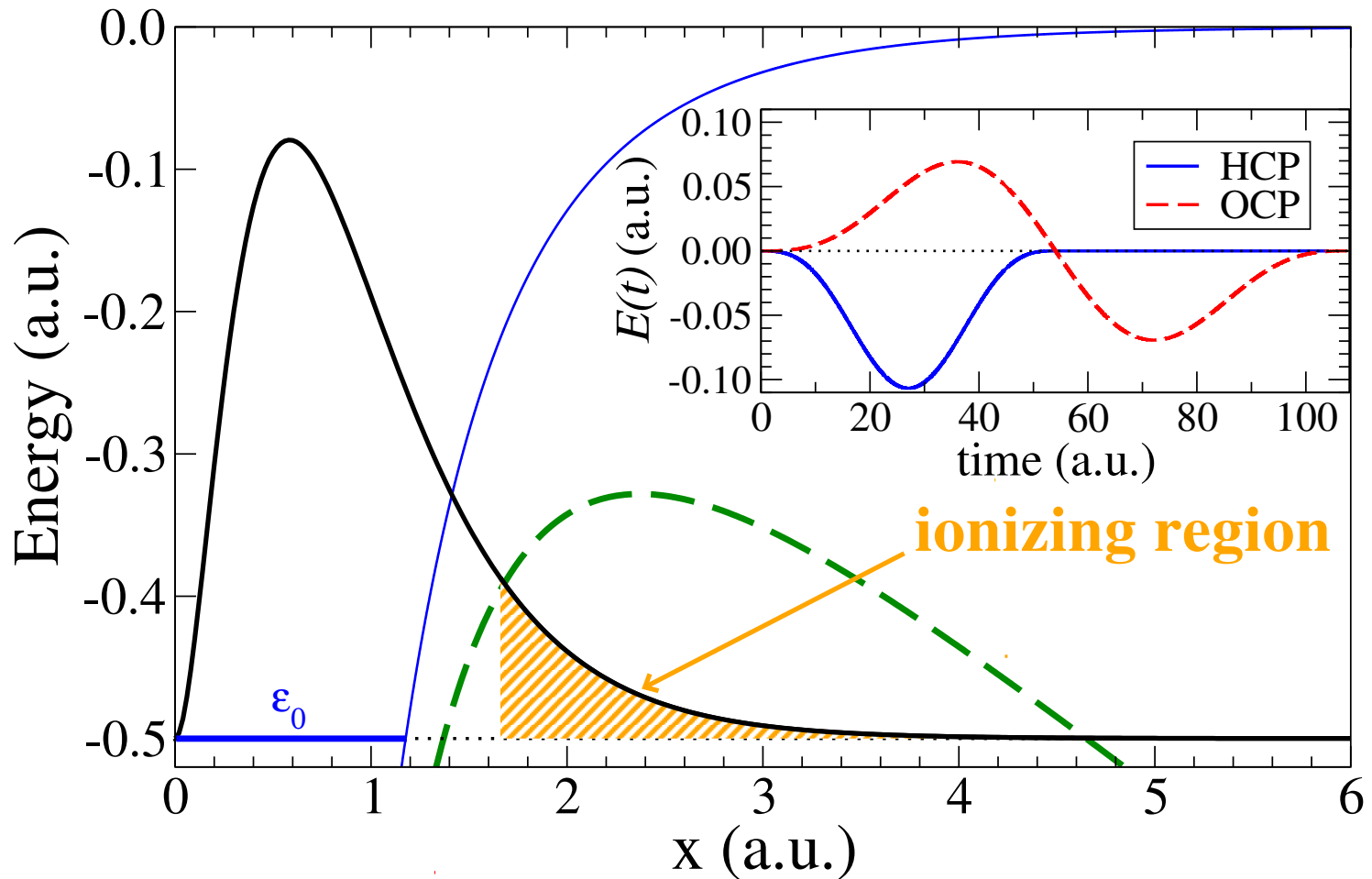
Department of Physics and Astronomy, Drake University, Des Moines, Iowa 50311, USA

(Dated: April 21, 2017)

Recent attoclock experiments and theoretical studies revealed new features in the strong-field ionization of atoms by few-cycle infrared light, thereby raising the need for an improved description of tunneling ionization. We consider a one-dimensional problem to thoroughly investigate the underlying mechanism in tunneling ionization. In the major part of the below-the-barrier ionization region, in an intense half-cycle or one-cycle infrared pulse, the electron does not tunnel “through” the barrier, but rather starts from the classically forbidden region. We highlight a remarkable correspondence between the probability of locating the electron in a particular initial position and its asymptotic momentum. Finally, Bohmian mechanics provides a natural definition of a mean tunneling time and exit position, taking into account the time-dependent nature of the barrier.

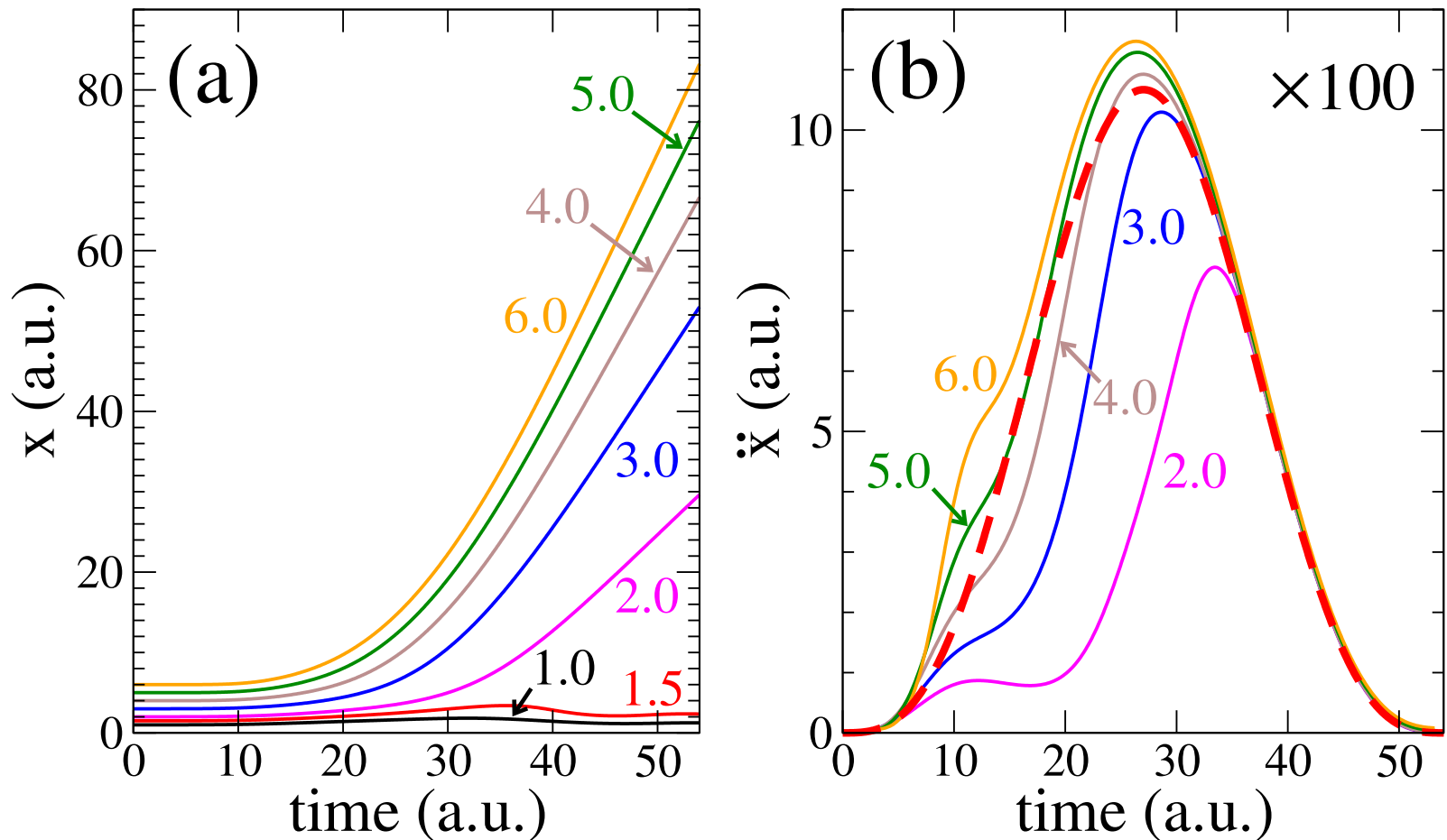
The next few slides show the main results for the 1D Yukawa potential and half- or one-cycle pulses.

Escaping from the classically forbidden region ...



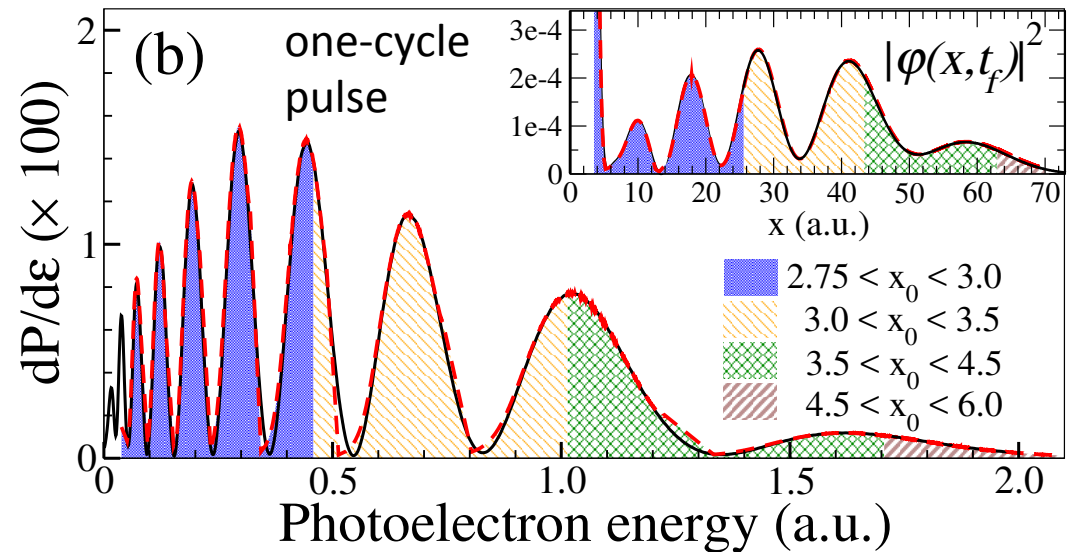
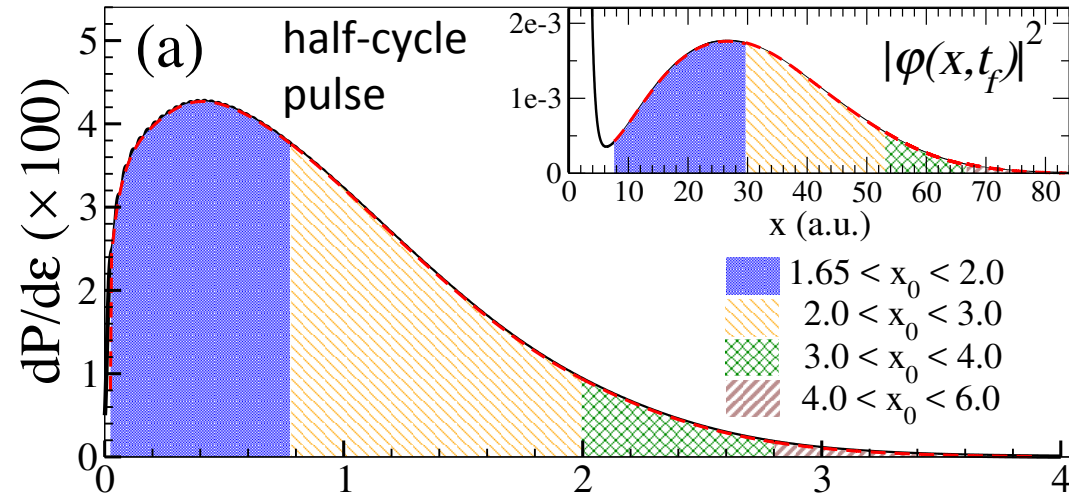
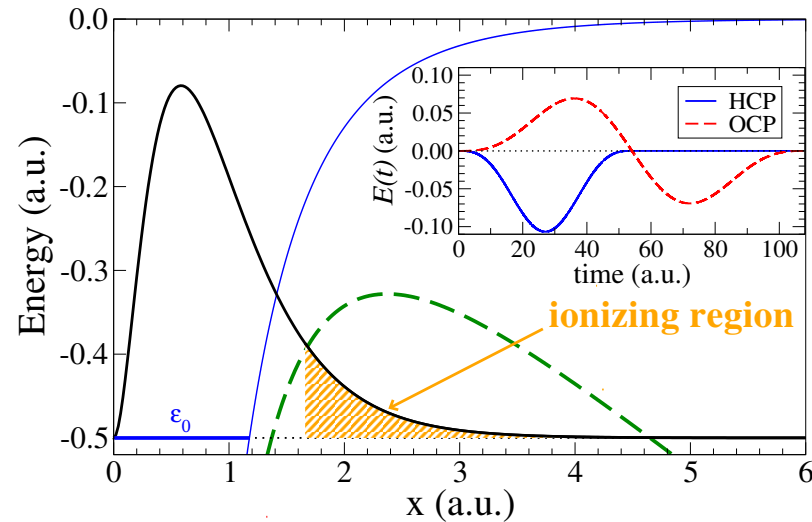
thin solid blue line: field-free 1D Yukawa potential
green dashed line: potential at maximum field (4×10^{14} W/cm²)
thick black line: ground state probability distribution.

Bohmian Trajectories and Acceleration



Trajectories starting in the classically allowed region return.
Consequently, the electron would not get out!

Initial Position vs. Final Energy



- The quantum-mechanical and Bohmian spectra are almost indistinguishable.
- Each final energy range can be associated with a range of starting values.
- For **multi-cycle pulses**, each ATI peak is expected to be traceable back to a starting range.

Conclusions from Bohmian Mechanics

- It is unlikely for electrons to tunnel through the entire barrier, unless the intensity gets close to the “over the barrier” value.
- Many of the free electrons seen after the pulse will likely have started already in the classically forbidden regime.

Conclusions from Bohmian Mechanics

- It is unlikely for electrons to tunnel through the entire barrier, unless the intensity gets close to the “over the barrier” value.
- Many of the free electrons seen after the pulse will likely have started already in the classically forbidden regime.
- Bohmian Mechanics also provides a tool to investigate tunneling times and exit points. [See our manuscript for details.]
- These ideas, and their consequences, need to be studied in more realistic cases than in 1D.

Conclusions from Bohmian Mechanics

- It is unlikely for electrons to tunnel through the entire barrier, unless the intensity gets close to the “over the barrier” value.
- Many of the free electrons seen after the pulse will likely have started already in the classically forbidden regime.
- Bohmian Mechanics also provides a tool to investigate tunneling times and exit points. [See our manuscript for details.]
- These ideas, and their consequences, need to be studied in more realistic cases than in 1D.
- It is hoped that Bohmian Mechanics (a very popular approach recently) will be able to provide further insight regarding the understanding, and ultimately, **the control of ultrafast dynamics in atoms, molecules, and solids.**

Conclusions from Bohmian Mechanics

- **It is unlikely for electrons to tunnel through the entire barrier,** unless the intensity gets close to the “over the barrier” value.
- Many of the free electrons seen after the pulse will likely have started already in the classically forbidden regime.
- Bohmian Mechanics also provides a tool to investigate tunneling times and exit points. [See our manuscript for details.]
- These ideas, and their consequences, need to be studied in more realistic cases than in 1D.
- It is hoped that Bohmian Mechanics (a very popular approach recently) will be able to provide further insight regarding the understanding, and ultimately, **the control of ultrafast dynamics in atoms, molecules, and solids.**

THANK YOU FOR YOUR ATTENTION!
(and our many collaborators for their contributions)